Review of Comparative Medicine 2008

Douglas K Taylor, DVM, DACLAM

C.L. Davis NC State

May 8, 2009

Doug's Quick Tips

- Read *everything* and take notes
  - Least emphasis on materials and methods
  - Subsequently study only the notes
- Focus on facts that you think you can actually remember (606 pages in 2008 Comp Med-you gotta cut bait at times)
- Try to formulate a few reasonable questions from any given paper
  - Bear in mind that the exam questions must be backed by 2 references
- Think about papers in 2 ways:
  - Is there data from the paper that might serve as a question?
  - Does the paper serve to prompt a question about older, classic core material?

Volume 58 (1)
February, 2008

Special Issue: Infectious Diseases in Nonhuman Primates

Introduction

Beyond Specific Pathogen-Free: Biology and Effect of Common Viruses in Macaques

Nicholas W Lerche[1] and Joe H Simmons[2,*]

Macaque models have contributed to key advances in our basic knowledge of behavior, anatomy, and physiology as well as to our understanding of a wide variety of human diseases. This issue of *Comparative Medicine* focuses on several of the viral agents (members of *Retroviridae*, *Herpesviridae* and 2 small DNA viruses) that can infect both nonhuman primates and humans as well as confound research studies. Featured articles also address the challenges of developing colonies of macaques and other nonhuman primates that are truly specific pathogen-free for these and other adventitious infectious agents.

Abbreviations: SPF, specific pathogen free; SV40, *Simian virus 40*

Overviews

Monkey B Virus (*Cercopithecine herpesvirus 1*)

David Elmore[1] and Richard Eberle[2,*]

Macaques are a particularly valuable nonhuman primate model for a wide variety of biomedical research endeavors. B virus (*Cercopithecine herpesvirus* 1; BV) is an α-herpesvirus that naturally infects conventional populations of macaques. Serious disease due to BV is rare in macaques, but when transmitted to humans, BV has a propensity to invade the central nervous system and has a fatality rate greater than 70% if not treated promptly. The severe consequences of human BV infections led to the inclusion of BV in the original NIH list of target viruses for elimination by development of specific pathogen-free rhesus colonies. In macaques and especially in humans, diagnosis of BV infection is not straightforward. Furthermore, development and maintenance of true BV specific pathogen-free macaque colonies has proven difficult. In this overview we review the natural history of BV in macaques, summarize what is known about the virus at the molecular level, and relate this information to problems associated with diagnosis of BV infections and development of BV-free macaque colonies.

Abbreviations: BSL, Biosafety Level; BV, B virus (*Cercopithecine herpesvirus 1*); ChHV, chimpanzee herpesvirus; HSV, herpes simplex virus; HVP2, *Herpesvirus papio 2* (*Cercopithecine herpesvirus 16*); HVS1, *Herpesvirus saimiri 1*; mAb, monoclonal antibody; ORF, open reading frame; RL, long repeat region; RS, short repeat region; SA8, simian agent 8 (*Cercopithecine herpesvirus 2*); SPF, specific pathogen free; CNS, central nervous system

Note

- Cercopithecine herpesvirus
  - Alphaherpesvirus
  - Related to: *herpesvirus saimiri, herpesvirus papio 2, herpes simplex*
- What alphaherpesvirus has been shown to be a suitable surrogate for b virus in serological diagnostic testing?

Note

- Cercopithecine herpesvirus
  - Alphaherpesvirus
  - Related to: *herpesvirus saimiri, herpesvirus papio 2, herpes simplex*
- What alphaherpesvirus has been shown to be a suitable surrogate for b virus in serological diagnostic testing?
  - *Herpesvirus papio 2*

Simian Varicella in Old World Monkeys

Wayne L Gray

Simian varicella virus (SVV) causes a natural erythematous disease in Old World monkeys and is responsible for simian varicella epizootics that occur sporadically in facilities housing nonhuman primates. This review summarizes the biology of SVV and simian varicella as a veterinary disease of nonhuman primates. SVV is closely related to varicella–zoster virus, the causative agent of human varicella and herpes zoster. Clinical signs of simian varicella include fever, vesicular skin rash, and hepatitis. Simian varicella may range from a mild infection to a severe and life-threatening disease, and epizootics may have high morbidity and mortality rates. SVV establishes a lifelong latent infection in neural ganglia of animals in which the primary disease resolves, and the virus may reactivate later in life to cause a secondary disease corresponding to herpes zoster. Prompt diagnosis is important for control and prevention of epizootics. Antiviral treatment for simian varicella may be effective if administered early in the course of infection.

Abbreviations: FEAU, 1-(2′-deoxy-2′-flouro-β-D-arabinofuranosyl)-5-iodouracil; IE, immediate early; ORF, open reading frame; PBL, peripheral blood lymphocyte; SVV, simian varicella virus; VZV, varicella–zoster virus

Note

- Lots of taxonomy
  - Cercopithecoidea, Cercopithecinae
  - *Chlorocebus aethiops, Erythrocebus patas, Pan troglodytes, Pongo pygmaeus*
- Virus
  - Alphaherpesvirus, *Varicellovirus, Cercophithecine herpesvirus 9*
  - Closely related to *human herpesvirus 3* (varicella-zoster)
  - Various isolates (page 23)

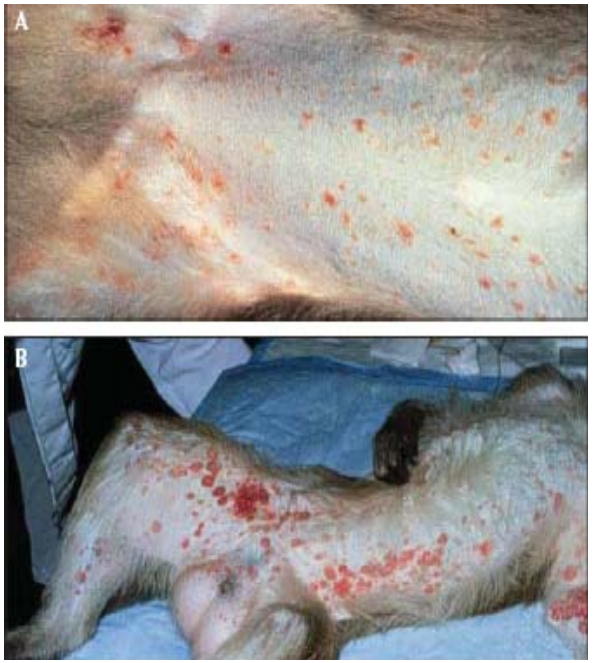

Comparative Pathobiology of Kaposi Sarcoma-associated Herpesvirus and Related Primate Rhadinoviruses

Susan V Westmoreland and Keith G Mansfield*

With the emergence of the AIDS epidemic over the last 2 decades and the more recent identification of Kaposi sarcoma-associated herpesvirus (KSHV, *Human herpesvirus 8*), the genera of rhadinoviruses have gained importance as a family of viruses with oncogenic potential. First recognized in New World primates more than 30 y ago, the rhadinoviruses *Saimiriine herpesvirus 2* and *Ateline herpesvirus 2* have well-described transforming capabilities. Recently several new species-specific rhadinoviruses of Old World primates have been described, including retroperitoneal fibromatosis herpesvirus and rhesus rhadinovirus (*Cercopithecine herpesvirus 17*). Molecular analysis of these viruses has elucidated several functionally conserved genes and properties shared with KSHV involved in cellular proliferation, transformation, and immune evasion that facilitate the oncogenic potential of these viruses. This review examines the comparative pathobiology of KSHV, discusses the role of macaque rhadinoviruses as models of human disease, and outlines the derivation of specific pathogen-free animals.

Development of Breeding Populations of Rhesus Macaques (*Macaca mulatta*) That Are Specific Pathogen-free for Rhesus Cytomegalovirus

Peter A Barry[1–3,*] and Lisa Strelow[1]

Development of breeding colonies of rhesus macaques (*Macaca mulatta*) that are specific pathogen-free (SPF) for rhesus cytomegalovirus (RhCMV) is relatively straightforward and requires few modifications from current SPF programs. Infants separated from the dam at or within a few days of birth and cohoused with similarly treated animals remain RhCMV seronegative indefinitely, provided they are never directly or indirectly exposed to a RhCMV-infected monkey. By systematically cohousing seronegative animals into larger social cohorts, breeding populations of animals SPF for RhCMV can be established. The additional costs involved in expanding the current definition of SPF status to include RhCMV are incremental compared with the money already being spent on existing SPF efforts. Moreover, the large increase in research opportunities available for RhCMV-free animals arguably would far exceed the development costs. Potential new areas of research and further expansion of existing research efforts involving these newly defined SPF animals would have direct implications for improvements in human health.

Abbreviations: HCMV, human cytomegalovirus; NHP, nonhuman primate; RhCMV, rhesus cytomegalovirus; SPF, specific pathogen-free

Simian Parvoviruses: Biology and Implications for Research

Meredith A Simon

The simian parvoviruses (SPVs) are in the genus *Erythrovirus* in the family *Parvoviridae* and are most closely related to the human virus B19. SPV has been identified in cynomolgus, rhesus, and pigtailed macaques. All of the primate erythroviruses have a predilection for erythroid precursors. Infection, which is common in macaques, is usually clinically silent. Disease from SPV is associated with immunosuppression due to infection with various retroviruses (SIV, simian retrovirus, and simian–human immunodeficiency virus), surgery, drug toxicity studies, and posttransplantation immunosuppressive treatment and therefore is of concern in studies that use parvovirus-positive macaques.

Abbreviations: SHIV, chimeric simian–human immunodeficiency virus; SPV, simian parvovirus; SRV, type D simian retrovirus; SIV, simian immunodeficiency virus

Polyomaviruses of Nonhuman Primates: Implications for Research

Meredith A Simon

Polyomaviruses are a family of small nonenveloped DNA viruses that infect birds and mammals. At least 7 nonhuman primate polyomaviruses that occur in macaques, African green monkeys, marmosets baboons, and chimpanzees have been described, as well as 4 polyomaviruses that occur in humans. *Simian virus 40* (SV40), which infects macaques, was the first nonhuman primate polyomavirus identified as a contaminant of early polio vaccines. Primate polyomaviruses cause inapparent primary infections but persist in the host and can cause severe disease in situations of immunocompromise. This review describes the primate polyomaviruses, and the diseases associated with the viruses of macaques. In macaques, the greatest current concerns are the potential confounding of study results by polyomavirus infections and the zoonotic potential of SV40.

Abbreviations: PML, progressive multifocal leukoencephalopathy; SV40, *Simian virus 40*

Comparative Pathobiology of Macaque Lymphocryptoviruses

Angela Carville and Keith G Mansfield*

Lymphocryptoviruses (LCVs) have been identified as naturally occurring infections of both Old and New World nonhuman primates. These viruses are closely related to Epstein–Barr virus (EBV, *Human herpesvirus 4*) and share similar genomic organization and biological properties. Nonhuman primate LCVs have the ability to immortalize host cells and express a similar complement of viral lytic and latent genes as those found in EBV. Recent evidence indicates that nonhuman primate LCVs can immortalize B cells from genetically related species, suggesting a close evolutionary relationship between these viruses and their respective hosts. Early work with EBV in tamarins and owl monkeys revealed that cross species transmission of lymphocryptoviruses from the natural to inadvertent host may be associated with oncogenesis and the development of malignant lymphoma. Moreover, simian LCVs have the ability to induce malignant lymphomas in immunodeficient hosts and have been associated with posttransplantation lymphoproliferative disease in cynomolgus macaques undergoing solid organ transplantation. This review will focus on the comparative pathobiology of lymphocryptoviral infection and discuss the derivation of specific pathogen-free animals.

Abbreviations: EBER, EBV-encoded small RNA; EBNA, Epstein–Barr nuclear antigen; EBV, Epstein–Barr virus; LCV, lymphocryptovirus; LMP, latent membrane protein; NHL, non-Hodgkin lymphoma; PTLD, posttransplantation lymphoproliferative disease; RhLCV, rhesus LCV; SHIV, simian–human immunodeficiency virus; sVCA, small viral capsid antigen

- Non-Hodgkin lymphoma in SIV-infected macaques is associated with concurrent infection with what?:
  1. Gamma 1 herpesvirus
  2. Gamma 2 herpesvirus
  3. Alpha herpesvirus
  4. Beta herpesvirus
  5. All members of *herpesviridae*

- Non-Hodgkin lymphoma in SIV-infected macaques is associated with what agent?:
  1. **Gamma 1 herpesvirus (page 60/61)**
  2. Gamma 2 herpesvirus
  3. Alpha herpesvirus
  4. Beta herpesvirus
  5. All members of *herpesviridae*

Clinical and Pathologic Features of Cynomolgus Macaques (*Macaca fascicularis*) Infected with Aerosolized *Yersinia pestis*

Roger Van Andel,[1,4,*] Robert Sherwood,[1] Chris Gennings,[3] C Richard Lyons,[2] Julie Hutt,[1] Andrew Gigliotti,[1] and Ed Barr[1]

Since the anthrax attacks of 2001, the emphasis on developing animal models of aerosolized select agent pathogens has increased. Many scientists believe that nonhuman primate models are the most appropriate to evaluate pulmonary response to, vaccines for, and treatments for select agents such as *Yersinia pestis* (*Y. pestis*), the causative agent of plague. A recent symposium concluded that the cynomolgus macaque (*Macaca fascicularis*) plague model should be characterized more fully. To date, a well-characterized cynomolgus macaque model of pneumonic plague using reproducible bioaerosols of viable *Y. pestis* has not been published. In the current study, methods for creating reproducible bioaerosols of viable *Y. pestis* strain CO92 (YpCO92) and pneumonic plague models were evaluated in 22 Indonesian-origin cynomolgus macaques. Five macaques exposed to doses lower than 250 CFU remained free of any indication of plague infection. Fifteen macaques developed fever, lethargy, and anorexia indicative of clinical plague. The 2 remaining macaques died without overt clinical signs but were plague-positive on culture and demonstrated pathology consistent with plague. The lethal dose of plague in humans is reputedly less than 100 organisms; in this study, 66 CFU was the dose at which half of the macaques developed fever and clinical signs (ED_{50}), The Indonesian cynomolgus macaque reproduces many aspects of human pneumonic plague and likely will provide an excellent model for studies that require a macaque model.

Susceptibility of Owl Monkeys (*Aotus nancymaae*) to Experimental Infection with *Bartonella bacilliformis*

David E Bentzel,[1,*] Benjamin J Espinosa,[2] Enrique Canal,[2] David L Blazes,[3] and Eric R Hall[2]

Bartonellosis, caused by *Bartonella bacilliformis*, is a clinically significant disease in parts of South America, where it is characterized by fever and hemolytic anemia during the often-fatal acute stage and warty skin eruptions during chronic disease. In this study, we evaluated owl monkeys (*Aotus nancymaae*) as a potential model for studying the immunogenicity and pathology of bartonellosis. Two groups of animals (n = 3 per group) received either 9.5×10^7 CFU *B. bacilliformis* by the ID route or 1.1×10^6 CFU by the IV route and were followed for 140 d. Animals were evaluated by physical exam, complete blood count or hematocrit (or both); infection was confirmed by Giemsa staining of blood smears, PCR amplification, and blood culture. On days 7 and 21, Giemsa-stained blood smears from both groups contained organisms (1% to 4% of erythrocytes). All blood cultures and PCR tests were negative. Complete blood counts and chemistry panels showed no difference from baseline. Serology revealed a greater than 4-fold increase in the IgM titer (compared with baseline levels) in the 3 animals from the ID group and 1 animal from the IV group. On day 35, a dermal lesion was excised from the inguinal region of 1 monkey from each group, with a second lesion excised on day 84 from the same monkey in the IV group. However the histopathology and immunostaining of these samples were not consistent with *B. bacilliformis*. The present study shows that owl monkeys can be infected with *B. bacilliformis*, but additional dosage studies are necessary to evaluate the usefulness of this species as a disease model for human bartonellosis.

- *Aotus nancymaae*

- Giemsa staining

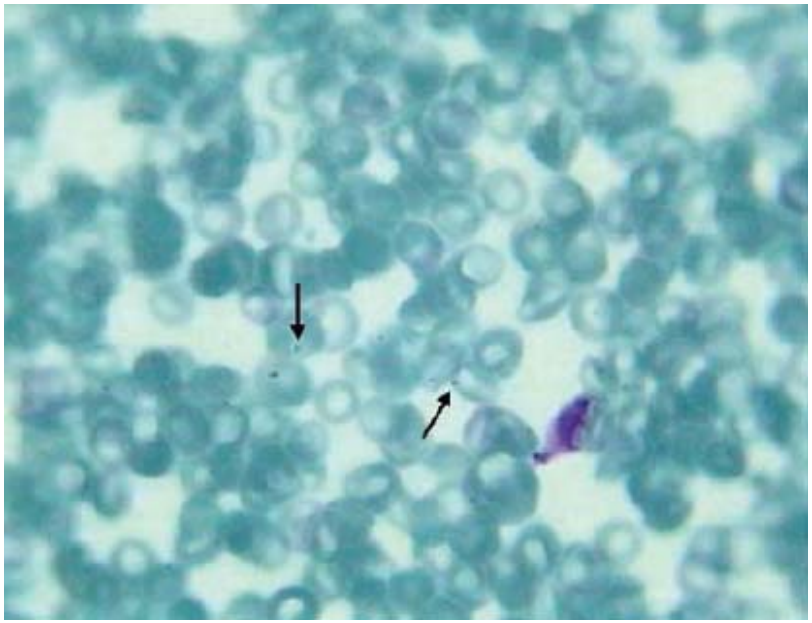

Effects of the Macrolide Drug Tylosin on Chronic Diarrhea in Rhesus Macaques (*Macaca mulatta*)

Rebecca S Blackwood,* Ross P Tarara, Kari L Christe, Abigail Spinner, and Nicholas W Lerche

Diarrhea is the gastrointestinal disease most frequently encountered in captive rhesus macaques. The precise pathogenic mechanisms underlying chronic diarrhea in nonhuman primates are not well understood, but a persistent inflammatory component has been implicated strongly. This study evaluated the inflammatory changes in the colon of macaques with diarrhea and assessed the efficacy of a 10-d course of tylosin in a cohort of 21 animals with chronic diarrhea. Stool quality was evaluated daily, and fecal consistency was scored. Colonoscopies were performed; biopsy samples were characterized histologically and assayed for expression of TNFα mRNA. Blood samples collected pre-, mid-, and post-treatment were assayed for C-reactive protein (CRP). The results indicated that 63% of the animals receiving tylosin showed improvement in stool quality, compared with 10% in the sham-treated group. Histologically, 82% of animals in the tylosin-treated group had a reduction in the severity of colonic lesions post-treatment, compared with 40% of animals in the sham group. The amount of TNFα mRNA before treatment did not differ from that afterward in either tylosin- or sham-treated animals. CRP levels serially decreased in tylosin-treated monkeys; the average post-treatment CRP value for tylosin-treated animals was 11.96 ± 3.86 μg/ml compared with 26.48 ± 4.86 μg/ml for sham-treated controls. In conclusion, tylosin significantly improved the fecal consistency score, significantly decreased colonic inflammation, and significantly decreased serum CRP levels post-treatment in rhesus macaques with chronic diarrhea.

Safety and Colonization of Two Novel *virG*(*icsA*)-based Live *Shigella sonnei* Vaccine Strains in Rhesus Macaques (*Macaca mulatta*)

Todd A Collins,* Shoshana Barnoy, Shahida Baqar, Ryan T Ranallo, Kevin W Nemelka, and Malabi M Venkatesan

Shigella are gram-negative bacterium that cause bacillary dysentery (shigellosis). Symptoms include diarrhea and discharge of bloody mucoid stools, accompanied by severe abdominal pain, nausea, vomiting, malaise, and fever. Persons traveling to regions with poor sanitation and crowded conditions become particularly susceptible to shigellosis. Currently a vaccine for *Shigella* has not been licensed in the United States, and the organism quickly becomes resistant to medications. During the past 10 y, several live attenuated oral *Shigella* vaccines, including the strain WRSS1, have been tested in humans with considerable success. These Phase I vaccines lack the gene for the protein VirG also known as IcsA, which enables the organism to disseminate in the host target tissue. However, 5% to 20% of the vaccinated volunteers developed mild fever and brief diarrhea, and the removal of additional virulence-associated genes from the vaccine strain may reduce or eliminate these side effects. We administered 2 *Shigella sonnei* vaccines, WRSs2 and WRSs3, along with WRSS1 to compare their rates of colonization and clinical safety in groups of 5 rhesus macaques. The primate model provides the most physiologically relevant animal system to test the validity and efficacy of vaccine candidates. In this pilot study using a gastrointestinal model of infection, the vaccine candidates WRSs2 and WRSs3, which have additional deletions in the enterotoxin and LPS modification genes, provided better safety and comparable immunogenicity to those of WRSS1.

Volume 58 (2)
April, 2008

Modeling Sepsis in the Laboratory: Merging Sound Science with Animal Well-Being

Jean A Nemzek,[1,*] Kelly MS Hugunin,[1] and Mark R Opp[2]

Despite impressive advances in biomedical research, few noteworthy breakthroughs have been made in the treatment of sepsis during the past several decades. This stalemate is primarily due to the intricate and heterogenic nature of the systemic immune responses characterized as the sepsis syndrome. In general, such complexity must be approached with in vivo models. Several animal models have been described, suggesting that none adequately address all of the pressing needs in sepsis research. The most clinically applicable models involve a localized infection, such as surgically induced polymicrobial sepsis, that gradually propagates a systemic immune response. Because relevant models must mimic a severe and chronic syndrome, animal well-being is often a concern in sepsis research. A balance between the needs of sepsis research and animal welfare can only be achieved through knowledge of the strengths and weaknesses of and alternatives to in vivo sepsis models.

Abbreviations: CASP, colon ascendens stent peritonitis; CLP, cecal ligation and puncture; LPS, lipopolysaccharide; TLR, Toll-like receptor

- Which of the following biomarkers can serve as a useful surrogate endpoint in models of sepsis?:
  1. Amyloid
  2. C-reactive protein
  3. IL-6
  4. IL-10
  5. Reactive nitric oxide species

- Which of the following biomarkers can serve as a useful surrogate endpoint in models of sepsis?:
  1. Amyloid
  2. C-reactive protein
  3. **IL-6 (page 126)**
  4. IL-10
  5. Reactive nitric oxide species

Intranasal Immunization with Recombinant Vesicular Stomatitis Virus Expressing Murine Cytomegalovirus Glycoprotein B Induces Humoral and Cellular Immunity

Steven R Wilson,[1,*] Jean H Wilson,[1] Linda Buonocore,[2] Amy Palin,[2,†] John K Rose,[2] and Jon D Reuter[1,††]

Cytomegalovirus is a leading cause of morbidity and mortality among neonatal and immunocompromised patients. The use of vaccine prophylaxis continues to be an effective approach to reducing viral infections and their associated diseases. Murine cytomegalovirus (mCMV) has proven to be a valuable animal model in determining the efficacy of newly developed vaccine strategies in vivo. Live recombinant vesicular stomatitis viruses (rVSV) have successfully been used as vaccine vectors for several viruses to induce strong humoral and cellular immunity. We tested the ability of intranasal immunization with an rVSV expressing the major envelope protein of mCMV, glycoprotein B (gB), to protect against challenge with mCMV in a mouse model. rVSV–gB-infected cells showed strong cytoplasmic and cell surface expression of gB, and neutralizing antibodies to gB were present in mice after a single intranasal vaccination of VSV–gB. After challenge with mCMV, recovery of live virus and viral DNA was significantly reduced in immunized mice. In addition, primed splenocytes produced a $CD8^+$ IFNγ response to gB. The ability to induce an immune response to a gene product through mucosal vaccination with rVSV–gB represents a potentially effective approach to limiting CMV-induced disease.

Abbreviations: CMV, cytomegalovirus; gB, glycoprotein B; h, human; m, murine; rVSV, recombinant vesicular stomatitis virus

- Which of the following characterizes cytomegaloviruses?:
  1. ssDNA gammaherpesvirus
  2. ssDNA alphaherpesvirus
  3. ssDNA betaherpesvirus
  4. dsDNA gammaherpesvirus
  5. dsDNA betaherpesvirus

- Which of the following characterizes cytomegaloviruses?:
  1. ssDNA gammaherpesvirus
  2. ssDNA alphaherpesvirus
  3. ssDNA betaherpesvirus
  4. dsDNA gammaherpesvirus
  5. **dsDNA betaherpesvirus (page 129)**

Transmission Probabilities of *Mouse Parvovirus 1* to Sentinel Mice Chronically Exposed to Serial Dilutions of Contaminated Bedding

David G Besselsen[1,*] Erin L Myers,[1] Craig L Franklin,[2] Scott W Korte,[2] April M Wagner,[1] Kenneth S Henderson,[3] and Benjamin J Weigler[4]

Intermittent serodetection of mouse parvovirus (MPV) infections in animal facilities occurs frequently when soiled bedding sentinel mouse monitoring systems are used. We evaluated induction of seroconversion in naïve single-caged weanling ICR mice (n = 10 per group) maintained on 5-fold serially diluted contaminated bedding obtained from SCID mice persistently shedding MPV1e. Soiled bedding from the infected SCID mice was collected, diluted, and redistributed weekly to cages housing ICR mice to represent chronic exposure to MPV at varying prevalence in a research colony. Sera was collected every other week for 12 wk and evaluated for reactivity to MPV nonstructural and capsid antigens by multiplex fluorescent immunoassay. Mice were euthanized after seroconversion, and DNA extracted from lymph node and spleen was evaluated by quantitative PCR. Cumulative incidence of MPV infection for each of the 7 soiled bedding dilution groups (range, 1:5 to 1:78125 [v/v]) was 100%, 100%, 90%, 20%, 70%, 60%, and 20%, respectively. Most seropositive mice (78%) converted within the first 2 to 3 wk of soiled bedding exposure, correlating to viral exposure when mice were 4 to 7 wk of age. Viral DNA was detected in lymphoid tissues collected from all mice that were seropositive to VP2 capsid antigen, whereas viral DNA was not detected in lymphoid tissue of seronegative mice. These data indicate seroconversion occurs consistently in young mice exposed to high doses of virus equivalent to fecal MPV loads observed in acutely infected mice, whereas seroconversion is inconsistent in mice chronically exposed to lower doses of virus.

Abbreviations: mfi, median fluorescent intensity; MFI, multiplex fluorescent immunoassay; MPV, mouse parvovirus; NS1, nonstructural protein 1; qPCR, quantitative PCR; SCID, severe combined immunodeficiency; VP2, viral capsid protein 2

Question

- Which of the following is the correct formula for calculating specificity?:
  1. TP/(TP + FN)
  2. TN/(TN + FP)
  3. FN/(TN + FP)
  4. TP/(TP + FP)
  5. TN/(TN + FN)

Question

- Which of the following is the correct formula for calculating specificity?:
  1. TP/(TP + FN)
  2. **TN/(TN + FP)**
  3. FN/(TN + FP)
  4. TP/(TP + FP)
  5. TN/(TN + FN)

Comparison of Tetraploid Blastocyst Microinjection of Outbred Crl:CD1(ICR), Hybrid B6D2F1/Tac, and Inbred C57BL/6NTac Embryos for Generation of Mice Derived from Embryonic Stem Cells

Sharron M Kirchain,[1,*] Alison M Hayward,[1] John M Mkandawire,[2] Peimin Qi,[1] and Aurora A Burds[2]

Embryo electrofusion and tetraploid blastocyst microinjection is a modification of the traditional embryonic stem cell (ES cell)-based method to generate targeted mutant mice. Viability of tetraploid embryos is reportedly lower than with diploid embryos, with considerable interstrain variation. Here we assessed fetus and pup viability after ES cell microinjection of tetraploid blastocysts derived from outbred, hybrid, and inbred mice. Two-cell mouse embryos (C57BL/6NTac [B6], n = 788; B6D2F1/Tac [BDF1], n = 1871; Crl:CD1(ICR) [CD1], n = 1308) were electrofused; most resultant tetraploid blastocysts were injected with ES cells and surgically transferred into pseudopregnant recipient mice. Reproductive tracts were examined at midgestation for embryologic studies using B6 and BDF1 blastocysts; implantation sites and viable fetuses were counted. Pregnancies were carried to term for studies of targeted mutant mice using BDF1 and CD1 blastocysts, and pup yield was evaluated. Electrofusion rates of 2-cell embryos did not differ among B6, BDF1, and CD1 mice (overall mean, 92.8% ± 5.4%). For embryologic studies, 244 B6 blastocysts were surgically transferred and 1 fetus was viable (0.41%), compared with 644 BDF1 blastocysts surgically transferred and 88 viable fetuses (13.7%). For targeted mutant mouse studies, 259 BDF1 blastocysts were surgically transferred yielding 10 pups (3.9%); 569 CD1 blastocysts yielded 44 pups (7.7%).

Abbreviations: B6, C57BL/6NTac; BDF1, B6D2F1/Tac; CD1, Crl:CD1(ICR); E, embryonic day; ES cell, embryonic stem cell; GFP, green fluorescent protein; KSOM-AA, potassium simplex optimized medium with amino acids

- Which of the following is an advantage of tetraploid blastocyst microinjection over diploid injection:?
  1. The tissues of tetraploid-derived animals arise from ES cells 25% of the time
  2. The tissues of tetraploid-derived animals arise from ES cells 50% of the time
  3. The tissues of tetraploid-derived animals arise from ES cells 100% of the time
  4. The tetraploid method requires less time
  5. The tetraploid method costs less initially

- Which of the following is an advantage of tetraploid blastocyst microinjection over diploid injection:?
  1. The tissues of tetraploid-derived animals arise from ES cells 25% of the time
  2. The tissues of tetraploid-derived animals arise from ES cells 50% of the time
  3. **The tissues of tetraploid-derived animals arise from ES cells 100% of the time (page 145)**
  4. The tetraploid method requires less time
  5. The tetraploid method costs less initially

High-carbohydrate Diets Affect the Size and Composition of Plasma Lipoproteins in Hamsters (*Mesocricetus auratus*)

Limin Wang,[1,†,*] Jun Yu,[2] and Rosemary L Walzem[1,2,*]

High-carbohydrate diets reduce plasma low-density lipoprotein (LDL)–cholesterol but also provoke the appearance of an atherogenic lipoprotein profile (ALP). Characterized by high plasma triglyceride, small dense LDL, and reduced high-density lipoprotein (HDL) cholesterol, an ALP is associated with insulin resistance. Despite extensive use of the fructose-fed hamster as a model of insulin resistance, little is known about changes that occur in the physical properties of circulating lipoproteins. Therefore, we investigated the metabolic and physical properties of lipoproteins in hamsters fed high-carbohydrate diets of varying complexity (60% carbohydrate as chow, cornstarch, or fructose) for 2 wk. Hamsters fed the high-fructose diet showed significantly increased very- low-density lipoprotein (VLDL)–triglyceride (92.3%), free cholesterol (68.6%), and phospholipid (95%), whereas apolipoprotein B levels remained unchanged. Median diameter of circulating VLDL was larger in fructose-fed hamsters (63 nm) than in cornstarch-fed hamsters. Fructose feeding induced a 42.5% increase LDL–triglyceride concurrent with a 20% reduction in LDL–cholesteryl ester. Compositional changes were associated with reduced LDL diameter. In contrast, fructose feeding caused elevations in all HDL fractions. The physical properties of apolipoprotein-B-containing lipoprotein fractions are similar between fructose-fed hamsters and humans with ALP. However, metabolism of high-density lipoprotein appears to differ in the 2 species.

Abbreviations: ALP, atherogenic lipoprotein profile; ApoB, apolipoprotein B; C, cholesterol; CE, esterified cholesterol; Fch, free cholesterol; HDL, high-density lipoprotein; LDL, low-density lipoprotein; PL, phospholipid; SREBP, sterol regulatory element binding protein; TG, triglyceride; VLDL, very-low–density lipoprotein

- The image to the right shows the result of SDS-PAGE stained with Coomassie blue. What do the bands represent?:
  1. DNA
  2. RNA
  3. mRNA
  4. Protein
  5. Amino Acids

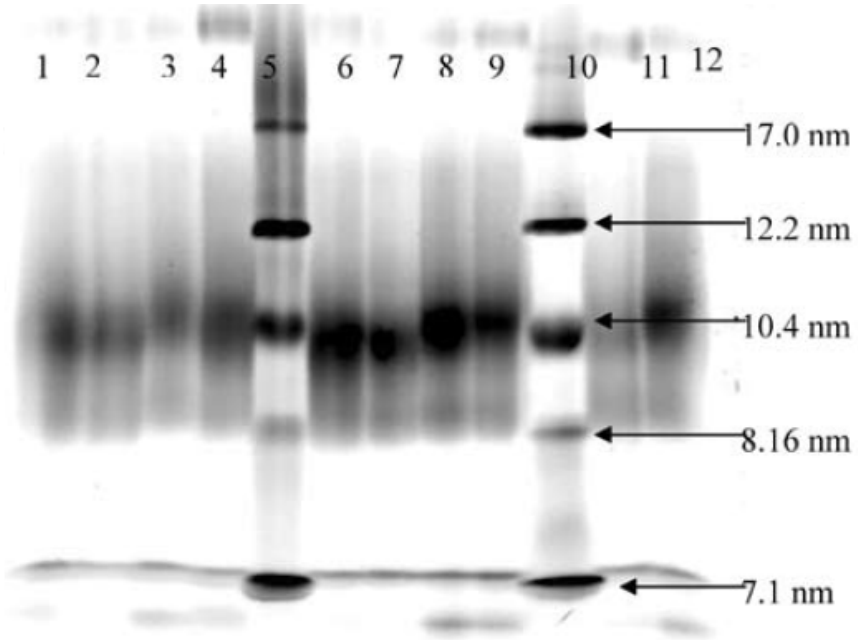

- The image to the right shows the result of SDS-PAGE stained with Coomassie blue. What do the bands represent?:
  1. DNA
  2. RNA
  3. mRNA
  4. **Protein (page 155)**
  5. IndividualAmino Acids

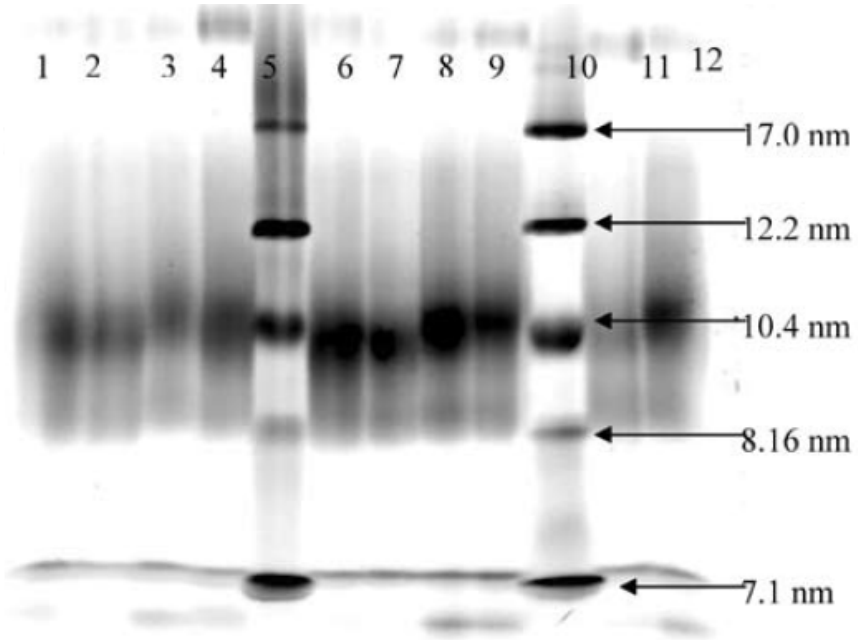

Cystic Renal Disease in the Domestic Ferret

Courtnye N Jackson, Arlin B Rogers, Kirk J Maurer, Jennifer LS Lofgren, James G Fox,* and Robert P Marini

Cystic renal diseases in domestic ferrets are a common anecdotal finding but have received scant systematic assessment. We performed a 17-y, case-control retrospective analysis of the medical records of 97 ferrets housed at our institution between 1987 and 2004, to determine the prevalence and morphotypes of cystic renal diseases in this species. Histologic sections stained with hematoxylin and eosin, Masson trichrome, or periodic acid–Schiff were evaluated by a comparative pathologist, and statistical analysis of hematologic and serum chemistry values was correlated with morphologic diagnosis. Of the 97 available records, 43 were eliminated due to lack of accompanying tissues. Of the 54 remaining cases, 37 (69% prevalence) had documented renal cysts, and 14 of the 54 ferrets (26%) had primary polycystic disease consisting of either polycystic kidney disease affecting renal tubules or, more commonly, glomerulocystic kidney disease. Secondary polycystic lesions were identified in 11 ferrets (20%), and 12 ferrets (22%) exhibited focal or isolated tubular cysts only as an incidental necropsy finding. Ferrets with secondary renal cysts associated with other developmental anomalies, mesangial glomerulopathy, or end-stage kidney disease had hyperphosphatemia and elevated BUN in comparison with those with primary cystic disease and elevated BUN compared with those without renal lesions. Although reflecting institutional bias, these results implicate primary and secondary cystic renal diseases as highly prevalent and underreported in the domestic ferret. In addition to the clinical implications for ferrets as research subjects and pets, these findings suggest a potential value for ferrets as a model of human cystic renal diseases.

Abbreviations: GCKD, glomerulocystic kidney disease; PKD, polycystic kidney disease

- Which of the following is NOT an animal model of polycystic kidney disease?:
  1. The Persian cat
  2. The Han:SPRD-cy rat
  3. The B6(Cg)-*Cys1*^{cpk}/J mouse
  4. The Long-Evans cinnamon rat
  5. C57BL/6J-*Nek8*^{jck}/J mouse

- Which of the following is NOT an animal model of polycystic kidney disease?:
  1. The Persian cat
  2. The Han:SPRD-cy rat
  3. The B6(Cg)-*Cys1*^{cpk}/J mouse
  4. **The Long-Evans cinnamon rat**
  5. The C57BL/6J-*Nek8*^{jck}/J mouse

Vascular-associated Lymphoid Tissue in Swine (*Sus scrofa*)

Ingeborg M Langohr,[1,*] Harm HogenEsch,[1] Gregory W Stevenson,[1] and Michael Sturek[2]

Focal accumulations of mononuclear cells in the arterial wall of healthy humans at predilection sites for atherosclerotic lesions have been described as 'vascular-associated lymphoid tissue' (VALT). Here we investigated whether pigs (*Sus scrofa*), a commonly used animal model for studying cardiovascular disease, have VALT. Samples of major arteries were collected from 10 conventional crossbred pigs (age, 2 to 24 mo) and processed for routine light microscopy, immunohistochemistry, and immunofluorescence. Single or small aggregates of mononuclear cells were noted in the intima and occasionally the inner portion of the tunica media and adventitia at branching sites. The infiltrating cells were primarily $CD3^+CD4^+$ T cells, with some macrophages. No $CD8^+$ T cells were present. Infiltrating leukocytes and overlying endothelial cells frequently expressed major histocompatibility class II molecules. Two Ossabaw pigs on low-fat diet had similar leukocytic aggregates at locations where animals of the same breed but fed a high-fat and high-cholesterol diet developed atherosclerotic lesions. Further, the densities of $CD3^+$ T lymphocytes and in these areas were decreased in 2 sedentary and 2 exercised Ossabaw pigs on an atherogenic diet compared with conventional crossbred and Ossabaw pigs on a normal diet. This study shows that focal aggregates of lymphocytes occur in the vasculature of pigs at locations predisposed to development of atherosclerotic lesions. These cellular aggregates are similar to the structures described as VALT in human arteries and reinforce the value of the pig as a model for the study of human cardiovascular disease.

Abbreviations: MAC387, myeloid–histiocytic antigen; MNC, mononuclear cells; TCR, T cell receptor; VALT, vascular-associated lymphoid tissue

- What type of cell predominates in the VALT of pigs and humans:?
  1. Monocytes
  2. CD4+ T lymphocytes
  3. CD8+ T lymphocytes
  4. B lymphocytes
  5. Neutrophils

- What type of cell predominates in the VALT of pigs and humans:?
  1. Monocytes
  2. **CD4+ T lymphocytes (page 171)**
  3. CD8+ T lymphocytes
  4. B lymphocytes
  5. Neutrophils

Porcine Models in Spinal Research: Calibration and Comparative Finite Element Analysis of Various Configurations during Flexion–Extension

Hadi N Aziz,[1,*] Fabio Galbusera,[1] Chiara Maria Bellini,[1] Giuseppe Vincenzo Mineo,[1,2] Alessandro Addis,[3] Riccardo Pietrabissa,[4] and Marco Brayda-Bruno[1]

This study was conducted to develop and calibrate a detailed 3-dimensional finite element model of the porcine lumbar spine and to compare this model with various configurations in flexion and extension. Computed tomography scans obtained from the L4–L5 lumbar segment of a Landrace × Large White pig were used to generate a solid volume. The various passive components were characterized by using a step-by-step calibration procedure in which the material properties of the anatomic structures were modified to match the corresponding in vitro data set-points retrieved from the literature. The range of motion of the totally assembled intact model was assessed under a 10-Nm flexion–extension moment and compared with data from a bilateral complete and hemifacetectomy configuration. In addition, the results from our porcine model were compared with published data regarding range of motion in a human finite element model in order to predict the configuration of the porcine model that most closely represented the human spine. Both the intact and hemifacetectomy configurations of the porcine model were comparable to the human spine. However, qualitative analysis of the instantaneous axis of rotation revealed a dissimilarity between the intact porcine model and human spine behavior, indicating the hemifacetectomy configuration of the porcine model as the most appropriate for spinal instrumentation studies. The present 3-dimensional finite element porcine model offers an additional tool to improve understanding of the biomechanics of the porcine spine and to decrease the expense of spinal research.

Abbreviations: CL, capsular ligament, FE, finite element; FJ, facet joint; IAR, instantaneous axes of rotation; ISL, interspinous ligament; IVD, intervertebral disc; LF, ligamentum flavum; RoM, range of motion; SSL, supraspinous ligament

Increased Production of 11β-hydroxysteroid Dehydrogenase Type 2 in the Kidney Microsomes of Squirrel Monkeys (*Saimiri* spp.)

Patti W Sadosky[2] and Jonathan G Scammell[1,2,*]

In squirrel monkeys (*Saimiri* spp.), cortisol circulates at levels much higher than those seen in man and other Old World primates, but squirrel monkeys exhibit no physiologic signs of the mineralocorticoid effects of cortisol. These observations suggest that squirrel monkeys have mechanisms for protection of the mineralocorticoid receptor (MR) from these high levels of cortisol. We previously showed that the serum cortisol to cortisone ratio in these animals is low relative to that in human serum, suggesting that production of the MR protective enzyme, 11β-hydroxysteroid dehydrogenase type 2 (11β-HSD2), is increased in squirrel monkeys. Here, we directly evaluate whether increased production of 11β-HSD2, which inactivates cortisol to cortisone, is a mechanism for protection of MR. In vitro assays showed that 11β-HSD2 activity in squirrel monkey kidney microsomes was 3 to 7 times higher than that seen in kidney microsomes from pig or rabbit. 11β-HSD2 protein detected by Western blot analysis was 4 to 9 times greater in squirrel monkey microsomes than in pig or rabbit microsomes. Comparison of the effect of expression of either human or squirrel monkey 11β-HSD2 on MR transactivation activity showed similar inhibition of MR response to cortisol by both enzymes, indicating that the intrinsic activities of the human and squirrel monkey enzymes are similar. These findings suggest that one mechanism by which squirrel monkeys protect the MR from activation by high cortisol levels in the kidney is by upregulation of 11β-HSD2 activity through increased production of the enzyme.

Abbreviations: 11β-HSD2, 11β-hydroxysteroid dehydrogenase type 2; CBX, carbenoxolone; MR, mineralocorticoid receptor

- Which species has circulating free cortisol levels up to 100x that of humans:?
  1. *Marmota monax*
  2. *Saimiri boliviensis*
  3. *Macaca mulatta*
  4. *Sigmodon hispidus*
  5. *Sus scrofa*

- Which species has circulating free cortisol levels up to 100x that of humans:?
  1. *Marmota monax*
  2. ***Saimiri boliviensis* (page 180)**
  3. *Macaca mulatta*
  4. *Sigmodon hispidus*
  5. *Sus scrofa*

Pathology of Captive Moustached Tamarins (*Saguinus mystax*)

Alfonso S Gozalo,[1,2,*] Lily I Cheng,[1,2] Marisa E St Claire,[3] Jerrold M Ward,[1,2] and William R Elkins[1]

The pathology of 33 moustached tamarins (*Saguinus mystax*) previously used in hepatitis A and GB virus studies is reported. Chronic lesions in colon, heart, and kidney were common in the monkeys and appeared not to be due to the experimental exposures. Colitis cystica profunda (CCP), a disease that affects humans and is characterized by the presence of mucin-filled epithelial downgrowths and cysts in the colonic submucosa, was found in 24 of the 33 (72.7%) tamarins. Interstitial myocardial fibrosis was present in 22 (66.6%) animals, and various degrees of membranoproliferative glomerulonephritis occurred in 28 (84.8%) monkeys. In addition, 28 (84.8%) tamarins demonstrated diffuse hepatocellular vacuolation with mild lymphoplasmacytic infiltrates, possibly as a result of the experimental infections, and peliosis hepatis occurred in 7 (21.2%) animals. The etiology of CCP is unknown, and no reliable animal models are available because most cases in animals are reported only sporadically. Myocardial fibrosis in tamarins has not been reported previously, and all current animal models require experimental manipulation of the animal to mimic the human disease. The results from this study suggest that captive *S. mystax* has high incidence of spontaneous CCP, myocardial fibrosis, and membranoproliferative glomerulonephritis. This species may be a spontaneous animal model for pathogenesis and experimental therapy studies of the analogous human diseases.

Abbreviation: CCP, colitis cystica profunda

- The tissue shown was stained with picrosirius red. This stain is specific for which of the following:?
  1. Amyloid
  2. Collagen
  3. Calcium
  4. Hemosiderin
  5. Lipid

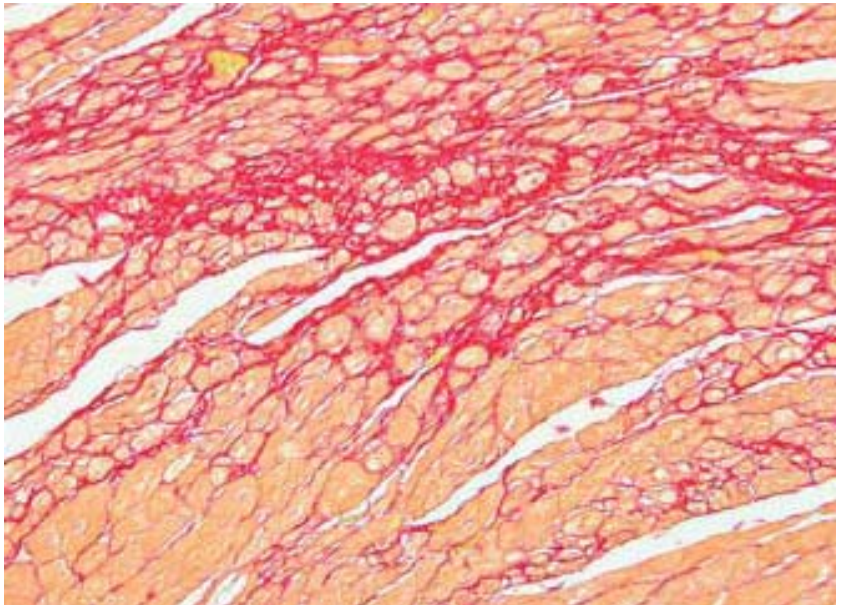

- The tissue shown was stained with picrosirius red. This stain is specific for which of the following:?

1. Amyloid
2. **Collagen (page 192)**
3. Calcium
4. Hemosiderin
5. Lipid

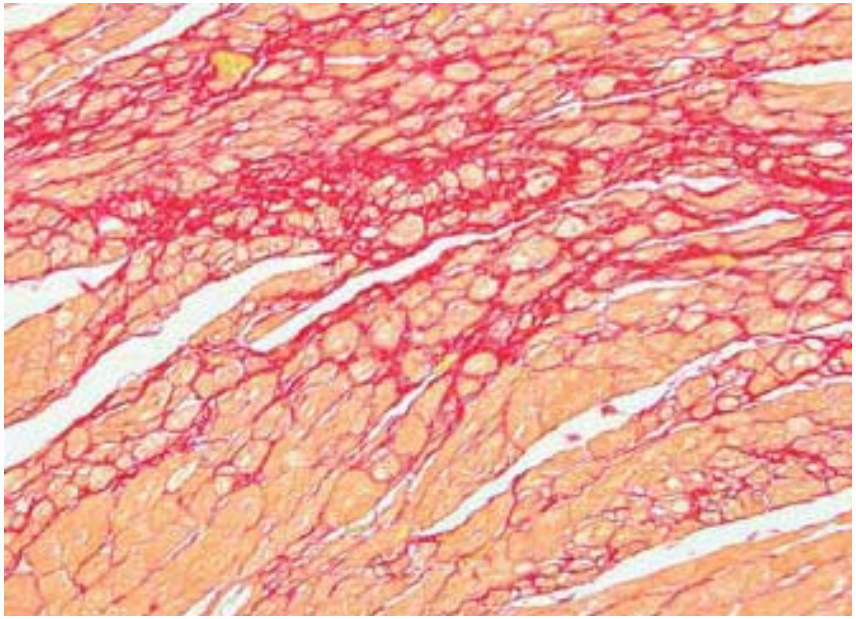

Volume 58(3)
June, 2008

Special Issue: Animal Models in the Study of Cancer

Animal Models of Cancer Pain

Cholawat Pacharinsak[1,*] and Alvin Beitz[2]

Modern cancer therapies have significantly increased patient survival rates in both human and veterinary medicine. Since cancer patients live longer they now face new challenges resulting from severe, chronic tumor-induced pain. Unrelieved cancer pain significantly decreases the quality of life of such patients; thus the goal of pain management is to not only to alleviate pain, but also to maintain the patient's physiological and psychological well-being. The major impediment for developing new treatments for cancer pain has been our limited knowledge of the basic mechanisms that drive cancer pain and the lack of adequate animal cancer pain models to study the molecular, biochemical and neurobiological pathways that generate and maintain cancer pain. However this situation has recently changed with the recent development of several novel animal models of cancer pain. This review will focus on describing these animal models, many of them in rodents, and reviewing some of the recent information gained from the use of these models to investigate the basic mechanims that underlie the development and maintenance of cancer pain. Animal models of cancer pain can be divided into the following five categories: bone cancer pain models, non-bone cancer pain models, cancer invasion pain models, cancer chemotherapeutic-induced peripheral neuropathy models, and spontaneous occurring cancer pain models. These models will be important not only for enhancing our knowledge of how cancer pain is generated, but more importantly for the development of novel therapeutic regimes to treat cancer pain in both domestic animals and humans.

Abbreviations: COX2, cyclooxygenase 2; DRG, dorsal root ganglion; NSAID, nonsteroidal antiinflammatory drug; TRPV1, transient receptor potential vanilloid 1

- Allodynia is defined as which of the following?:
  1. Lack of response to painful stimuli
  2. Exaggerated response to painful stimuli
  3. Response to noxious stimuli ameliorated by analgesia
  4. Response to non-noxious stimuli
  5. Response to noxious stimuli despite analgesia administration

- Allodynia is defined as which of the following?:
  1. Lack of response to painful stimuli
  2. Exaggerated response to painful stimuli
  3. Response to noxious stimuli ameliorated by analgesia
  4. **Response to non-noxious stimuli (page 222)**
  5. Response to noxious stimuli despite analgesia administration

- The image shown depicts what?:
  1. Hot plate testing
  2. Shock testing
  3. Aversion testing
  4. Conditioned response testing
  5. von Frey testing

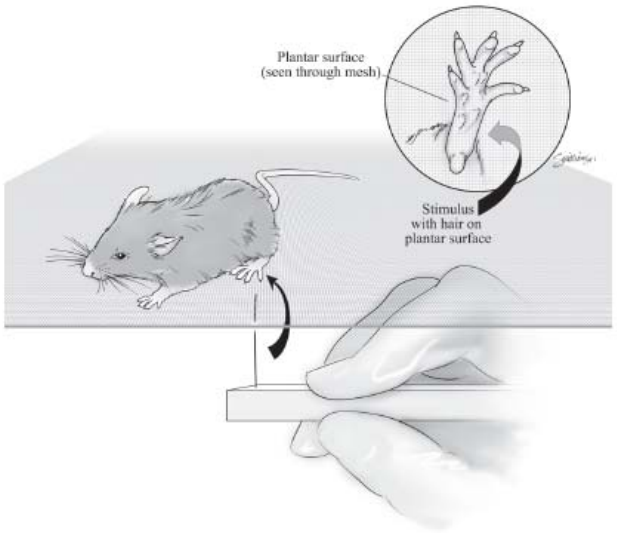

- The image shown depicts what?:
  1. Hot plate testing
  2. Shock testing
  3. Aversion testing
  4. Conditioned response testing
  5. **von Frey testing**

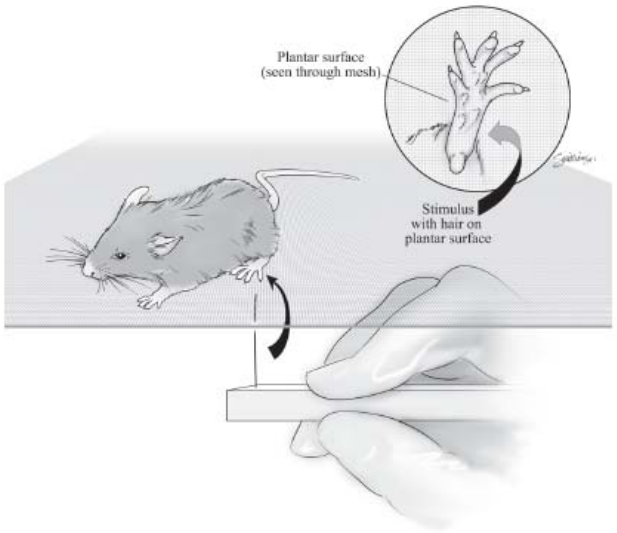

Fatigue and Sleep during Cancer and Chemotherapy: Translational Rodent Models

Maria Ray,[1] Laura Q Rogers,[2] Rita A Trammell,[2] and Linda A Toth[3,*]

The frequent occurrence of fatigue and disturbed sleep in cancer survivors and the negative effect of these symptoms on quality of life and clinical outcome underscore the need to identify mechanisms that cause cancer-related fatigue, with a view toward developing more effective treatments for this problem. Human studies of fatigue and disturbed sleep are limited by high interindividual genetic and environmental variability, difficulties with behavioral or reporting compliance, and the subjective nature of the problems. Although animal models also must overcome the barrier of assessing fatigue and sleep disturbance in the absence of obvious objective clinical markers, animal studies are easier to control and standardize than are studies of people. Moreover, animal models are crucial to the identification and understanding of underlying disease mechanisms. This review describes the need for, the feasibility of, and several possible approaches to measuring fatigue in animal models of cancer and to relating such measures to disturbed sleep, immune function, and other potential mechanisms. Developing and using animal models to better understand fatigue and disturbed sleep related to cancer and its treatment has an enormous potential to expand the knowledge base and foster hypotheses necessary for the future development and testing of interventions.

Abbreviations: HR-QOL, health-related quality of life; LLC1, Lewis lung carcinoma 1

- What cells are functional in mice that are homozygous for a mutation in the *Prkdc* gene?:
  1. T lymphocytes only
  2. B lymphocytes only
  3. T and B lymphocytes
  4. Natural killer cells
  5. T lymphocytes and antigen presenting cells

- What cells are functional in mice that are homozygous for a mutation in the *Prkdc* gene?:
  1. T lymphocytes only
  2. B lymphocytes only
  3. T and B lymphocytes
  4. **Natural killer cells (page 240)**
  5. T lymphocytes and antigen presenting cells

- A graft can be defined as “syngeneic” when:
  1. The donor and recipient are the same species, but different genotype
  2. The donor and recipient are the same species of the same genotype
  3. The donor and recipient are different species
  4. The donor and recipient are the same gender
  5. The donor and recipient are littermates

- A graft can be defined as “syngeneic” when:
  1. The donor and recipient are the same species, but different genotype
  2. **The donor and recipient are the same species of the same genotype (page 240)**
  3. The donor and recipient are different species
  4. The donor and recipient are the same gender
  5. The donor and recipient are littermates

Utility of AntiPax5 in the Diagnosis of Lymphoproliferative Disorders and Neoplasia in Mice

Jerold E Rehg[1,*] and John P Sundberg[2]

CD45R/B220 antigen (B220) is a common mouse panB-cell marker used for paraffin-embedded tissues. However, antiB220 has limited specificity in diagnostic pathology because the B220 antigen is expressed on subsets of cytotoxic T lymphocytes and natural killer cells, on plasmacytic dendritic cells, and on T lymphocytes of mice with the lymphoproliferative disorder associated with Fas (lymphoproliferative mutant mouse, B6.MRL-*Fas*^{lpr}/J) or Fas ligand (generalized lymphoproliferative disease mutant mouse, C3H/HeJ-*Fasl*^{gld}/J or B6Smn.C3-*Fasl*^{gld}/J). In addition, mouse B lymphocytes vary in the amount of B220 expressed, and some subsets of mouse B lymphocytes do not express B220 at all. In comparison, Pax5 expression (detected by immunohistochemistry using antiPax5) offers greater specificity and sensitivity because of its earlier expression during B-cell differentiation, its ability to detect all committed B cells, and its restriction to the B-cell lineage. Here we describe the use of an antibody to human Pax5 in diagnostic pathology with formalin-fixed, paraffin-embedded mouse tissue.

Abbreviations: B200, CD45R/B220 antigen; IHC, immunohistochemistry; LBL-NOS, lymphoblastic lymphoma, not otherwise specified; SJCRH, St Jude Children's Research Hospital; SMZL, splenic marginal zone lymphoma; Tdt, terminal deoxynucleotidyl transferase

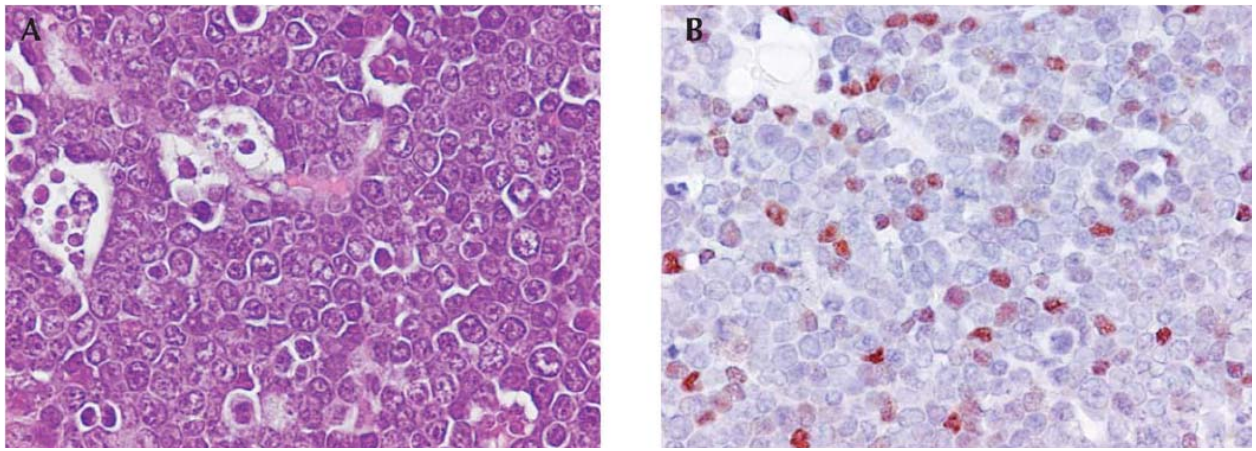

- This image shows a lymph node processed for histology (A) and immunohistochemistry (B). The brown cells in (B) are:
  1. Undergoing apoptosis
  2. Mutated
  3. Not expressing the targeted antigen
  4. Expressing the targeted antigen
  5. Macrophages

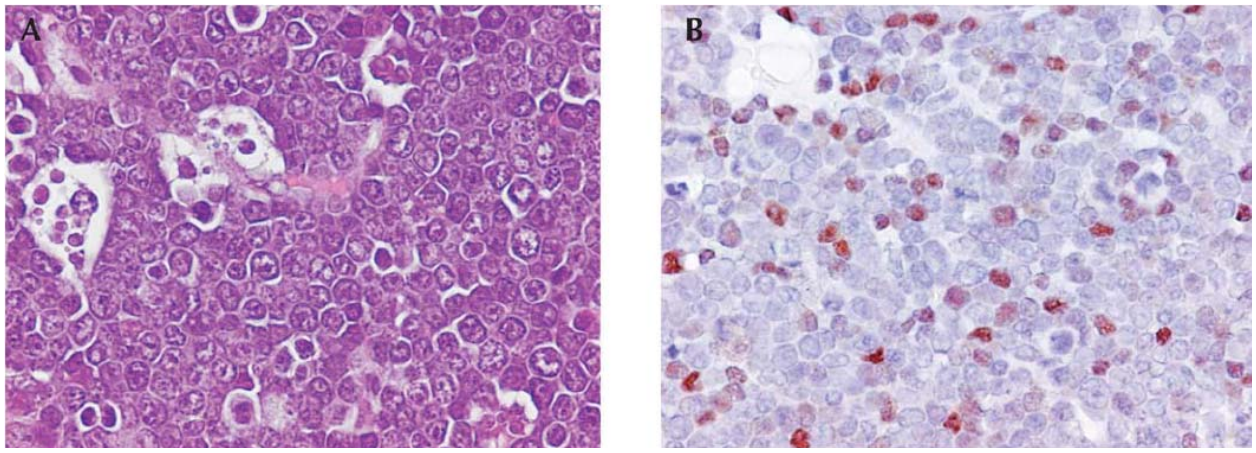

- This image shows a lymph node processed for histology (A) and immunohistochemistry (B). The brown cells in (B) are:
  1. Undergoing apoptosis
  2. Mutated
  3. Not expressing the targeted antigen
  4. **Expressing the targeted antigen (Page 250)**
  5. Macrophages

Histopathologic Findings and Establishment of Novel Tumor Lines from Spontaneous Tumors in FVB/N Mice

Peigen Huang,* Dan G Duda, Rakesh K Jain, and Dai Fukumura

The inbred FVB mouse strain is used extensively in cancer research. Transgenic mice with an FVB/N background in which the expression of green fluorescent protein is under the control of various promoters have been used widely for the last decade. However, little is known about the incidence and characteristics of spontaneous tumors in these mice. In addition, only a few tumor lines have been established for use in this particular mouse strain. Our aim was to initiate a database of spontaneous tumors in our retired FVB/N breeders, analyze the histopathologic characteristics of these tumors, and establish novel tumor lines in vivo and in vitro. A total of 234 (40 male, 194 female) breeder mice were observed during their natural lifespans. The incidence of spontaneous tumors was 45.0% in male mice and 52.8% in female mice. All tumors in male mice were lung alveolar–bronchiolar (AB) neoplasms, except for 1 testis interstitial cell tumor. In female mice, histopathologic examination revealed 48 lung AB tumors, 27 mammary gland tumors, 13 ovarian tumors, and 14 other tumors. Several of these spontaneous tumors have been transplanted into FVB/N mice. One mammary adenocarcinoma (MCaP0008) and 1 lung AB carcinoma (LAP0297) were successfully transplanted subcutaneously and passaged serially in vivo. Subsequently, we established cell lines from both tumors, which were maintained in monolayer in vitro. Both of the grafted tumors and cell lines are tumorigenic in *VEGF^{P}-GFP*/FVB and *Tie2^{P}-GFP*/FVB mice. Establishment of these novel tumor lines will benefit both in vivo and in vitro studies on the pathophysiology of cancer in this relatively new but widely used mouse strain.

Abbreviations: AB, alveolar–bronchiolar; GFP, green fluorescence protein; VEGF, vascular endothelial growth factor

- The FVB/N mouse strain exhibits what characteristic that makes it popular for genetic manipulation?:
  1. Large pronuclei in the zygote
  2. Favorable response to superovulation
  3. Large oocytes
  4. Large litters
  5. Higher than average DNA integration into the germline

- The FVB/N mouse strain exhibits what characteristic that makes it popular for genetic manipulation?:
  1. **Large pronuclei in the zygote (page 253)**
  2. Favorable response to superovulation
  3. Large oocytes
  4. Large litters
  5. Higher than average DNA integration into the germline

- The most common tumor found in aged, male FVB/N mice is what?:
  1. Squamous cell carcinoma
  2. Hepatocellular carcinoma
  3. Testicular interstitial cell tumor
  4. Alveolar-bronchiolar lung tumor
  5. Pituitary adenoma

- The most common tumor found in aged, male FVB/N mice is what?:
  1. Squamous cell carcinoma
  2. Hepatocellular carcinoma
  3. Testicular interstitial cell tumor
  4. **Alveolar-bronchiolar lung tumor (page 256)**
  5. Pituitary adenoma

A Structured Light-based System for Scanning Subcutaneous Tumors in Laboratory Animals

Ibrahim Cem Girit,[1,*] Maria Jure-Kunkel,[2] and Kim W McIntyre[3]

Tumor size or volume is often the primary endpoint in preclinical efficacy studies of anticancer drugs. Efficient and accurate measurement of such tumors is crucial to rapid evaluation of novel drug candidates. Currently available techniques for acquiring high-throughput data on tumor volume are time-consuming and prone to various inaccuracies and errors. The laser-scanning technology we describe here provides a convenient, high-throughput system for tumor measurement that reduces interoperator variability and bias while providing automated data collection, processing and analysis.

Abbreviations: 3D, 3-dimensional

Spontaneous Vulvar Papillomas in a Colony of Mice Used for Pancreatic Cancer Research

Naomi M Gades,[1,*] Akihiro Ohashi,[2] Lisa D Mills,[2] Matt A Rowley,[2] Kelly S Predmore,[3] Ronald J Marler,[4] and Fergus J Couch[2]

Mice in a colony used for pancreatic cancer research and maintained in a barrier animal facility presented with vulvar masses. A census and examination of all colony animals was conducted on 17 February 2006; line, gender, and mass location were recorded; a slide caliper was used to measure the width, length, and height of each mass; and the volume of each mass was calculated. Progeny female mice from crossbreeding of the B6.FVB-Tg(Ipf1-cre)1Tuv and B6;129-Kras2tm4Tyj ($KRAS^{G12D/+}$) strains presented with external vulvar and periauricular papillomas. The papillomas were present in 41.2% of all female crossbred mice and ranged in size from 8 to 36 mm^3. Age of mice and tumor size were not correlated. Compared with the B6.FVB-Tg(Ipf1-cre)1Tuv line, the crossbred female mice were more likely to have a vulvar mass, with an odds ratio of 29.3, 95% confidence interval (1.5, 563.9) and a positive predictive value of 42.9%. Diagnostic evaluation, including electron microscopy, light microscopy, serology, and bacteriology, did not reveal a viral or other infectious etiology. Therefore, we speculate that interaction between the genetic background of the mice and the introduced *Kras* oncogene may be responsible for these papillomas.

- The B6;129-*Kras2*^{tm4Tyj} mouse is used to study pancreatic cancer. What does the "**;**" indicate?
  1. Coisogenic
  2. Congenic
  3. Outbred
  4. Mixed background
  5. F1 hybrid

- The B6;129-*Kras2*^{tm4Tyj} mouse is used to study pancreatic cancer. What does the "**;**" indicate?

1. Coisogenic
2. Congenic
3. Outbred
4. **Mixed background**
5. F1 hybrid

Magnetic Resonance Imaging of the Response of a Mouse Model of Non-Small Cell Lung Cancer to Tyrosine Kinase Inhibitor Treatment

Xiangzhi Zhou,[1,*] Haihua Bao,[1] Ruqayyah Al-Hashem,[1] Hongbin Ji,[2] Mitchell Albert,[1] Kwok-Kin Wong,[2] and Yanping Sun[1]

Mutational activation of the gene for epidermal growth factor receptor (*EGFR*) is 1 of the main ways by which this receptor induces non-small cell lung cancers (NSCLC). Variant III EGFR (*EGFRvIII*) is a potential therapeutic target in NSCLC treatment because of the high frequency of deletion mutations in this protein. This study used noninvasive magnetic resonance imaging (MRI) to investigate the role of an *EGFRvIII* mutant in lung tumorigenesis and tumor maintenance as well as its response to the EGFR small molecule inhibitor erlotinib (Tarceva) on bitransgenic mice. Both spin-echo and gradient-echo sequences with and without cardiac and respiratory gating were performed to image the invasive mouse lung tumor driven by *EGFRvIII* mutation. Tumor volumes were measured based on 2-dimensional axial MRI; 3-dimensional rendering of the images were obtained to demonstrate the spatial location and distribution of the tumor in the lung. The MRI results indicated that the tumor driven by the *EGFRvIII* mutation was generated and maintained in the bitransgenic mice with the use of doxycycline. Tumor monitoring via MRI showed that Erlotinib can significantly inhibit the growth of tumor in vivo. MRI has the ability to image mouse lung tumor with different sequences focusing on tissue contrasts between tumor and surroundings. The MRI approaches in this work can be applied on other antitumor drug treatment evaluation in vivo when appropriate sequences are chosen.

Abbreviations: EGFR, epidermal growth factor receptor; GEFI, gradient-echo fast imaging; MRI, magnetic resonance imaging; NSCLC, non-small cell lung cancer; *EGFRvIII*, variant III *EGFR*; RARE, rapid acquisition relaxation–enhanced;

- The insertion of a tetracycline response element into the genome of a mouse allows for what?:
  1. Inducible gene expression
  2. Tissue specific gene expression
  3. Mutation of a gene
  4. Transgene insertion
  5. Chimera formation

- The insertion of a tetracycline response element into the genome of a mouse allows for what?:
  1. **Inducible gene expression (page 277)**
  2. Tissue specific gene expression
  3. Mutation of a gene
  4. Transgene insertion
  5. Chimera formation

- What imaging modality was used to create the image shown?
  1. Micro CT
  2. Micro PET
  3. MRI
  4. Ultrasound
  5. Radiography

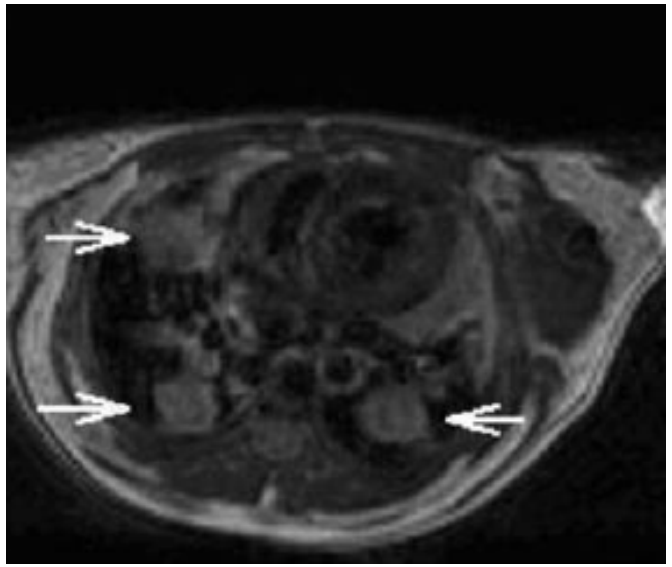

- What imaging modality was used to create the image shown?
  1. Micro CT
  2. Micro PET
  3. **MRI (page 278)**
  4. Ultrasound
  5. Radiography

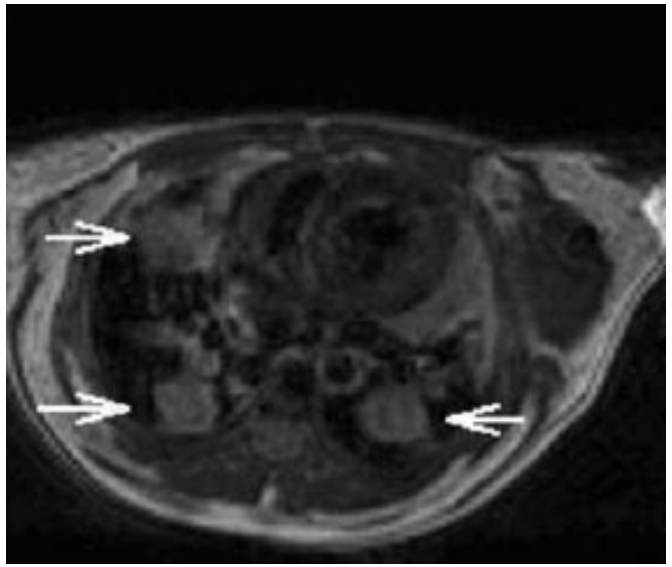

Rat Prostate Tumors Express Cancer Procoagulant, an Activator of Coagulation Factor X

Malgorzata Kamocka,[1,4,*] Morris Pollard,[2] Mark Suckow,[3] Wojciech P Mielicki,[1] and Elliot D Rosen[4]

Two common procoagulant activities associated with tumors are tissue factor and cancer procoagulant (CP), an activator of coagulation factor X. We have identified a convenient source of CP in transplanted Lobund–Wistar rat PA3 prostate tumors. CP activity was purified from 5 independent transplanted prostate tumors by column chromatography. The protein activated factor X in the absence of TF and factor VII. An antihuman CP antibody recognized rat CP in an ELISA and inactivated CP activity in a chromogenic assay. Lobund–Wistar prostate tumors may provide a convenient animal model useful in determining the role of CP in cancer development.

Abbreviations: CP, cancer procoagulant; FVII, coagulation factor VII; FX, coagulation factor X; LW, Lobund-Wistar rat; NMU, N-nitroso-N-methylurea; PAR, protease-activated receptor; TF, tissue factor

- Which of the following is a unique feature of the prostate cancer that develops in the Lobund-Wistar rat?:
  1. Only the ventral lobe is involved
  2. Only the lateral lobes is involved
  3. Only the anterior lobe is involved
  4. Only the ventral and lateral lobes are involved
  5. The ventral, lateral, and anterior lobes are all involved

- Which of the following is a unique feature of the prostate cancer that develops in the Lobund-Wistar rat?:
  1. Only the ventral lobe is involved
  2. Only the lateral lobes is involved
  3. Only the anterior lobe is involved
  4. Only the ventral and lateral lobes are involved
  5. **The ventral, lateral, and anterior lobes are all involved (page 282)**

Development of a Rabbit Pleural Cancer Model by Using VX2 Tumors

Kelly A. Kreuter,[1] Naglaa El-Abbadi,[1] Alia Shbeeb,[1] Lillian Tseng,[1] Sari Brenner Mahon,[1] Navneet Narula,[3] Tanya Burney,[1] Henri Colt,[2] and Matthew Brenner[1,2,*]

Primary and secondary pleural cancer remains an important clinical problem, with research progress limited by the lack of a suitable moderate- to large-sized (3 to 4 kg) animal model of pleural cancer. Many potential pleura-based imaging and treatment modalities cannot be investigated sufficiently by using currently available small murine animal models because their pleural space is not comparable to that of humans and therefore does not allow for the use of standard thoracoscopic techniques. Here we describe the development of a reproducible model of pleural malignancy in moderate-sized immunocompetent rabbits. Under thoracoscopic guidance, 9–15 × 10^6 VX2 carcinoma cells were inoculated into the plural space of 3 to 4 kg New Zealand white rabbits that had undergone gentle pleural abrasion. Malignant tumor involvement developed on the visceral and parietal pleural surfaces in an average of 2 to 4 wk. This novel pleural tumor model induction method likely will facilitate a broad range of investigations of pleural cancer diagnostics and therapeutics.

Spontaneous Fibrosarcoma in a Djungarian Hamster (*Phodopus sungorus*)

Hirotaka Kondo,[1] Mamoru Onuma,[1] Hidetoshi Ito,[1] Hisashi Shibuya[1], and Tsuneo Sato[1,*]

A 1.5-y-old female Djungarian hamster (*Phodopus sungorus*) presented with a large subcutaneous mass surrounding the right shoulder. Radiography revealed dislocation of the right humeral articulation and osteolytic lesions of the right scapula. Histologically, the mass was composed of spindle to stellate cells arranged in fascicles interwoven with delicate collagen fibers, and neoplastic cells infiltrated the bone, skeletal muscle, and subcutaneous tissues. Neoplastic cells stained intensely positive for vimentin and negative for S100 protein, neurofilament, and desmin. A minority of neoplastic cells (10% to 20%) stained moderately for smooth muscle actin. The mass was diagnosed as a fibrosarcoma. Although fibrosarcomas are relatively common in dogs and cats, this is the first report of fibrosarcoma in a domestic Djungarian hamster.

Abbreviations: D hamster, Djungarian hamster; GL cells, ganglion cell-like cells; SMA, smooth muscle actin

Note

- Djungarian hamster factoids
  - *Phodopus sungorus*
  - Shortest reproductive cycle of any eutherian species
  - High incidence of neoplasia-useful model
- Masson's trichrome: collagen
- Alcian blue stain: mucopolysaccharides and glycosaminoglycans
- Vimentin immunohistochemistry

Cystic Mammary Adenocarcinoma Associated with a Prolactin-secreting Pituitary Adenoma in a New Zealand White Rabbit (*Oryctolagus cuniculus*)

Paul Sikoski,[*,†] James Trybus, J Mark Cline, F Salih Muhammad, Andrew Eckhoff, Josh Tan, Mandy Lockard, Tammy Jolley, Susan Britt, and Nancy D Kock

A 44-mo-old, female, nulliparous New Zealand White Rabbit (*Oryctolagus cuniculus*) presented with bilaterally diffusely enlarged mammary glands with enlarged, discolored teats that exuded brown, mucoid discharge. The complete blood count and serum chemistry panels were within normal limits, bacteria were not isolated from a culture of the discharge, and the clinical signs did not resolve with antibiotic treatment. Computed tomography and serum prolactin levels supported the diagnosis of mammary gland dysplasia, possibly due to a prolactin-secreting pituitary adenoma. Histologic evaluation confirmed the presence of a pituitary adenoma, mammary hyperplasia, dysplasia, and cystic mammary adenocarcinoma. Immunohistochemical staining confirmed the presence of abundant prolactin secreting cells in the pituitary adenoma. This is the second report of hyperprolactinemia with mammary dysplasia in rabbits, and the first report of cystic mammary adenocarcinoma associated with a prolactin-secreting pituitary adenoma in a rabbit.

Note

- CT imaging

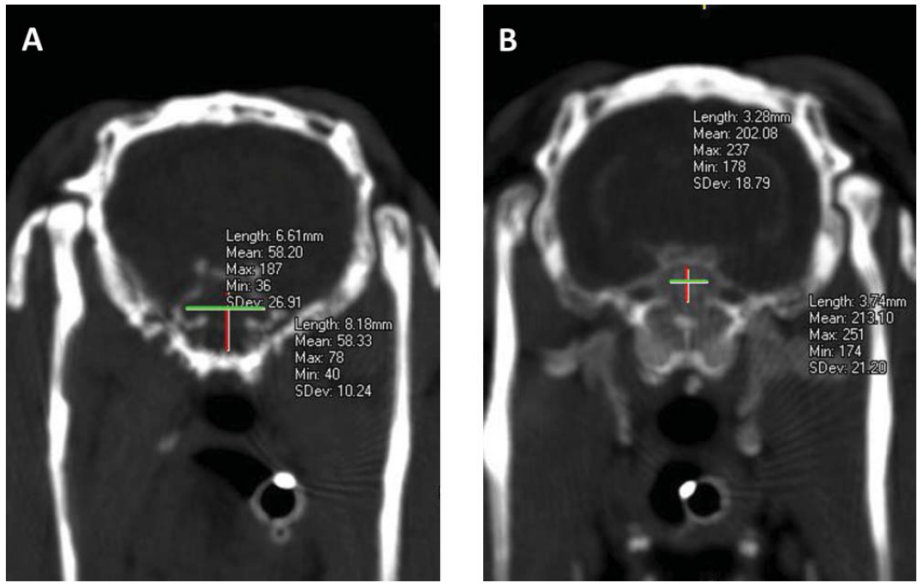

- Immunohistochemistry

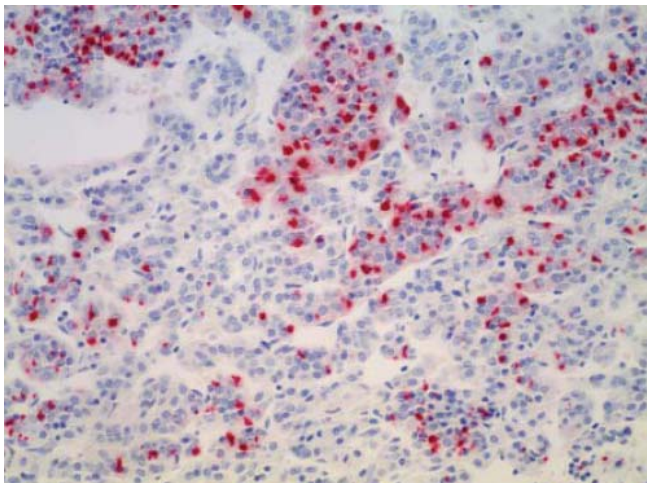

Volume 58(4)
August, 2008

The Guinea Pig as a Model of Infectious Diseases

Danielle J Padilla-Carlin,[1] David N McMurray,[2] and Anthony J Hickey[1,*]

The words 'guinea pig' are synonymous with scientific experimentation, but much less is known about this species than many other laboratory animals. This animal model has been used for approximately 200 y and was the first to be used in the study of infectious diseases such as tuberculosis and diphtheria. Today the guinea pig is used as a model for a number of infectious bacterial diseases, including pulmonary, sexually transmitted, ocular and aural, gastrointestinal, and other infections that threaten the lives of humans. Most studies on the immune response to these diseases, with potential therapies and vaccines, have been conducted in animal models (for example, mouse) that may have less similarity to humans because of the large number of immunologic reagents available for these other species. This review presents some of the diseases for which the guinea pig is regarded as the premier model to study infections because of its similarity to humans with regard to symptoms and immune response. Furthermore, for diseases in which guinea pigs share parallel pathogenesis of disease with humans, they are potentially the best animal model for designing treatments and vaccines. Future studies of immune regulation of these diseases, novel therapies, and preventative measures require the development of new immunologic reagents designed specifically for the guinea pig.

Abbreviations: BCG, bacille Calmette–Guérin; C4D, fourth component of complement; CXCR1, IL8 chemokine receptor; DTH, delayed-type hypersensitivity; GPIC, guinea pig inclusion conjunctivitis; MHC, major histocompatibility complex; PLL, poly-L-lysine; TGFβ, transforming growth factor β; TNFα, tumor necrosis factor α

- The guinea pig inclusion conjunctivitis model is used to study what human pathogen?
  1. Enteric calicivirus
  2. Respiratory syncytial virus
  3. *Legionella pneumophila*
  4. *Chlamydia trachomatis*
  5. *Streptococcus pneumoniae*

- The guinea pig inclusion conjunctivitis model is used to study what human pathogen?
  1. Enteric calicivirus
  2. Respiratory syncytial virus
  3. *Legionella pneumophila*
  4. ***Chlamydia trachomatis*** **(page 327)**
  5. *Streptococcus pneumoniae*

- The guinea pig's response to vaccination with bacille Calmette-Guerin is best described as what?:
  1. Type I hypersensitivity
  2. Type II hypersensitivity
  3. Type III hypersensitivity
  4. Type IV hypersensitivity
  5. Innate immune response

- The guinea pig's response to vaccination with bacille Calmette-Guerin is best described as what?:
  1. Type I hypersensitivity
  2. Type II hypersensitivity
  3. Type III hypersensitivity
  4. **Type IV hypersensitivity (page 325)**
  5. Innate immune response

Alterations in Methylation and Expression Levels of Imprinted Genes *H19* and *Igf2* in the Fetuses of Diabetic Mice

Wei-Juan Shao,[1,†] Ling-Yun Tao,[2] Cheng Gao,[2] Jian-Yun Xie,[2,*] and Ru-Qian Zhao[1,*,†]

The study aimed to reveal alterations in expression and methylation levels of the growth-related imprinted genes *H19* and *Igf2* in fetuses of diabetic mice. Diabetes was induced in female mice by intraperitoneal injection of streptozotocin. DNA and total RNA were extracted from fetuses obtained from diabetic and control dams on embryonic day (E) 14. Real-time RT-PCR analysis revealed that the mRNA expression of *Igf2* in fetuses from diabetic mice was 0.65-fold of the control counterparts. Bisulfite genomic sequencing demonstrated that the methylation level of the *H19–Igf2* imprint control region was 19.1% higher in diabetic fetuses than in those of control dams. In addition, the body weight of pups born to diabetic dams was 26.5% lower than that of the control group. The results indicate that maternal diabetes can affect fetal development by means of altered expression of imprinted genes. The modified genomic DNA methylation status of imprinting genes may account for the change in gene expression.

Abbreviation: E, embryonic day

Note

- Streptozoticin-induced model
- Restriction endonucleases
- Real time PCR

Embryonic Stem Cells Derived from C57BL/6J and C57BL/6N Mice

Yoko Tanimoto,[1,†] Saori Iijima,[1,†] Yoshikazu Hasegawa,[1] Yuko Suzuki,[1] Yoko Daitoku,[1] Seiya Mizuno,[1] Taichiro Ishige,[1] Takashi Kudo,[1] Satoru Takahashi,[1] Satoshi Kunita,[1] Fumihiro Sugiyama,[1,*] and Ken-ichi Yagami[1]

Mouse embryonic stem (ES) cells with the C57BL/6 genetic background allow the generation of knockout mice without the need to backcross to C57BL/6. However, C57BL/6 ES cells whose pluripotency after homologous recombination has been confirmed are not yet available from public cell banks. To facilitate the use of ES cells derived from C57BL/6 sublines in both biologic and medical research, we demonstrated that the use of knockout serum replacement as a medium supplement and 8-cell blastomeres as recipient embryos allowed establishment of ES cells and production of germline chimeric mice, respectively. Under effective conditions, a large number of ES cell lines were established from C57BL/6J and C57BL/6N blastocysts. The majority of ES cells in many cell lines obtained from both strains showed a normal chromosome number. Germline chimeric mice were generated from C57BL/6J and C57BL/6N ES cells. Finally, the ES cell line B6J-S1^{UTR}, derived from C57BL/6J, was used for successful production of gene knockout mice. C57BL/6J ES (B6J-S1^{UTR} and B6J-23^{UTR}) and C57BL/6N ES (B6N-22^{UTR}) cells are available from the cell bank of the BioResource Center at RIKEN Tsukuba Institute (http://www.brc.riken.jp/lab/cell/english/).

Abbreviations: ES, embryonic stem; KSR, knockout serum replacement

Note

- Embryonic stem cells
- Back crossing
- Genetic background
- Chimeras
- Germline transmission
- Targeting vectors
- Homologous recombination

Embryo Transfer Rederivation of C.B-17/Icr-*Prkdc*^{scid} Mice Experimentally Infected with Mouse Parvovirus 1

David G Besselsen,[1-3,*] Melissa J Romero-Aleshire,[1] Stephanie J Munger,[3] Emily C Marcus,[1] Kenneth S Henderson,[4] and April M Wagner[1]

We determined whether embryos derived from C.B-17/Icr-*Prkdc*^{scid} (SCID) mice infected with mouse parvovirus (MPV) 1b and mated to MPV-naïve B6C3F1 mice would transmit virus to naïve recipient female mice and rederived progeny. Viral DNA was detected by quantitative PCR (qPCR) in lymphoid tissues, gonad, sperm, and feces of all MPV1b-inoculated SCID mice. Viral DNA was detected in 1 of 16 aliquots of embryos from infected male SCID mice and in 12 of 18 aliquots of embryos from infected female SCID mice. All recipient female mice implanted with embryos from infected SCID male mice and their progeny were negative by serology and qPCR. In contrast, 3 of 5 recipient female mice implanted with embryos from infected SCID female mice and 14 of 15 progeny mice from these recipients were seropositive by multiplex fluorescent immunoassay (MFI) for MPV capsid antigen (rVP2). All of these mice were negative by MFI for parvovirus nonstructural protein antigen (rNS1) and by qPCR, with the exception of 1 recipient female mouse that displayed weak rNS1 seroreactivity and low levels of MPV DNA in lymphoid tissues. Seroreactivity to rVP2 declined over time in all progeny mice from infected SCID female mice until all were seronegative by 20 wk of age, consistent with maternal antibody transfer. Given that the high levels of MPV contamination detected in our experimentally infected SCID mice are unlikely in naturally infected immunocompetent mice, these data indicate that embryo transfer rederivation is effective for the eradication of MPV from infected colonies.

Abbreviations: mfi, median fluorescent intensity; MFI, multiplex fluorescent immunoassay; MPV, mouse parvovirus; MVM, minute virus of mice; qPCR, quantitative polymerase chain reaction; rNS1, parvoviral nonstructural protein antigen; rVP2, MPV capsid antigen; SCID, severe combined immunodeficiency; SW, Swiss–Webster

- Which of the following regimens is typically used to induce superovulation in mice?:
  1. PMSG injection followed 48 hours later by hCG
  2. hCG injection followed 48 hours later by PMSG
  3. PMSG injection followed 48 hours later by FSH
  4. hCG injection followed 48 hours later by FSH
  5. PMGS injection followed 48 hours later by estrogen injection

- Which of the following regimens is typically used to induce superovulation in mice?:
  1. **PMSG injection followed 48 hours later by hCG (page 354)**
  2. hCG injection followed 48 hours later by PMSG
  3. PMSG injection followed 48 hours later by FSH
  4. hCG injection followed 48 hours later by FSH
  5. PMGS injection followed 48 hours later by estrogen injection

- Which of the following is true regarding murine parvovirus proteins?:
  1. VP2 is a non-structural protein that is highly conserved among parvoviruses
  2. NS1 is a non-structural protein that is highly conserved among parvoviruses
  3. VP2 is a capsid protein that is highly conserved among parvoviruses
  4. NS1 is a capsid protein that is highly conserved among parvoviruses
  5. NS1 is a non-structural protein that is very specific for each species of parvovirus

- Which of the following is true regarding murine parvovirus proteins?:
  1. VP2 is a non-structural protein that is highly conserved among parvoviruses
  2. **NS1 is a non-structural protein that is highly conserved among parvoviruses**
  3. VP2 is a capsid protein that is highly conserved among parvoviruses
  4. NS1 is a capsid protein that is highly conserved among parvoviruses
  5. NS1 is a non-structural protein that is very specific for each species of parvovirus

Minute Virus of Mice: Antibody Response, Viral Shedding, and Persistence of Viral DNA in Multiple Strains of Mice

Lydia M Janus,[1,*] Michael Mähler,[2] Wiebke Köhl,[2] Anna Smoczek,[1] Hans J Hedrich,[1] and Andre Bleich[1]

Minute virus of mice (MVM) is a major concern for laboratory animal facilities because it remains with considerably high prevalence despite strict barrier systems. The aim of this study was to elucidate potential risks associated with MVM infection by investigating the role of the genetic background on antibody production and persistence as well as viral shedding. Mice of various strains and stocks were inoculated oronasally with the immunosuppressive strain MVMi; in addition, natural infection was modeled through contact exposure. As determined by serology, seroconversion and serum levels of IgG differed considerably among strains and stocks, especially in the contact-exposed group. For example, C57BL/6J mice responded well to exposure in contrast to FVB/N, NMRI, ICR, and C3H/HeN mice. Titration studies indicated that the viral dose necessary to induce seroconversion was strain-dependent. Experiments to dissect the role of the major histocompatibility complex haplotype in the response to MVMi gave inconclusive results. To detect viral persistence, spleens and feces were analyzed by PCR at 16 wk after exposure, and the infectivity of PCR-positive spleens was investigated by IP and oronasal inoculation of naive mice. Although DNA was detected in the spleens of some mice, feces remained negative, and naive mice were not infected by inoculation. In addition, viral shedding declined rapidly after day 20 postinoculation. In summary, the data show that seroconversion and antibody response to MVMi infection depend on the genetic background of mice, with the infective dose being a critical factor. The role of viral DNA in chronically infected mice will require further elucidation.

Abbreviations: B6, C57BL/6J; BQ, B10/Q-H2q/SgAi; ICR, CRL:CD1 ICR; IFA, immunofluroescent assay; MHC, major histocompatibility complex; MPV, mouse parvovirus; MVM, minute virus of mice; NS, nonstructural protein; VP, virion protein

- Which mouse strain exhibits a robust antibody response upon contact exposure to MVM?
  1. FVB/N
  2. ICR
  3. DBA/2J
  4. BALB/C
  5. C57BL/6

- Which mouse strain exhibits a robust antibody response upon contact exposure to MVM?
  1. FVB/N
  2. ICR
  3. DBA/2J
  4. BALB/C
  5. **C57BL/6 (page 363)**

Note

- Strain specificity of Th1 versus Th2 immune response
- Strains of mice: DBA/2, BALB/C, FVB/N, AKR…
- MHC haplotype
- Parvovirus antigens…again

An Acute Osteomyelitis Model in Traumatized Rat Tibiae Involving Sand as a Foreign Body, Thermal Injury, and Bimicrobial Contamination

James C McPherson III,[1,*] Royce R Runner,[2] Brian Shapiro,[2,3] Douglas S Walsh,[1] Julie Stephens-DeValle,[1] and Thomas B Buxton[2]

The multfactorial nature of bone injuries in modern warfare and emergency trauma patients warrants enhancement of existing models. To develop a more appropriate model, rat tibiae (n = 195) were mechanically injured, divided into 2 groups (with or without thermal injury), and contaminated with a range of *Staphylococcus aureus* (Cowan 1) inocula. In some experiments, *S. aureus* inocula also contained *Escherichia coli* or foreign bodies (sand or soil). The primary outcome measure was the amount of *S. aureus* remaining in the tibia (tibial bacterial load) 24 h after contamination, reported as $\log_{10}$ cfu/g bone. *S. aureus* showed ID_{50} and ID_{95} values of 72 and 977 cfu, respectively. Values were lower than seen previously by using *S. aureus* strain SMH. *S. aureus* tibial bacterial loads were higher in tibiae with mechanical and thermal injury ($\log_{10}$ 4.15 ± 0.27 cfu/g) versus mechanical injury alone ($\log_{10}$ 3.1 ± 0.47 cfu/g, $P = 0.028$). The addition of *E. coli* to the *S. aureus* inoculum had no effect on tibial bacterial loads (*S. aureus* only, $\log_{10}$ 4.24 ± 0.92 cfu/g; *S. aureus* + *E. coli*, $\log_{10}$ 4.1 ± 1.0 cfu/g, $P = 0.74$). Sand, added as a foreign body, increased tibial bacterial load. Combined mechanical and thermal trauma of the tibia is associated with increased *S. aureus* tibial bacterial loads, increasing the risk of acute osteomyelitis. Understanding the interplay of mechanical and thermal injuries, bimicrobial contamination, and foreign bodies may improve our understanding of traumatic bone injuries and the pathogenesis of osteomyelitis.

P26-based Serodiagnosis for *Bartonella* spp. Infection in Cats

Jonathan A Werner,[1] Sunlian Feng,[1] Bruno B Chomel,[2] Emir Hodzic,[1] Rickie W Kasten,[2] and Stephen W Barthold[1,*]

Bartonella henselae P26 has been identified as an immunodominant antigen expressed during feline infection. We used antisera from cats experimentally infected with *B. henselae* (n = 6), *B. clarridgeiae* (n = 4), or *B. koehlerae* (n = 2) and from a sample of naturally infected cats (*B. henselae*, n = 34; *B. clarridgeiae*, n = 1) to evaluate recombinant P26 (rP26) as a serodiagnostic antigen. Immunoblots using antisera from cats infected with *B. henselae* and *B. clarridgeiae* reacted strongly with rP26, whereas *B. koehlerae* antisera did not. A capture ELISA was designed to evaluate the kinetics of rP26 IgG in sera from experimentally infected cats. For *B. henselae* and *B. clarridgeiae* antisera, the kinetic profiles of reactivity were similar for rP26 capture ELISA and *Bartonella* spp. indirect fluorescence assay. However, for *B. koehlerae* antisera, reactivity in rP26 capture ELISA was consistently low. The serodiagnostic potential of rP26 capture ELISA was evaluated using sera from cats with known *Bartonella sp.* exposure histories. All 24 (100%) uninfected cats were seronegative, and 33 of 35 (94.3%) cats bacteremic for *Bartonella* spp. were seropositive. We propose that rP26-based serology can serve as a useful adjunct tool for the diagnosis of feline infection with *B. henselae* and *B. clarridgeiae*, but it may not be useful for feline infection with *B. koehlerae*.

Abbreviations: RFLP, restriction fragment length polymorphism; rP26, recombinant P26

Note

- *Bartonella henselae* = cat scratch disease causative agent
- Western blot
- Capture ELISA
- RFLP analysis
- PCR
- IFA

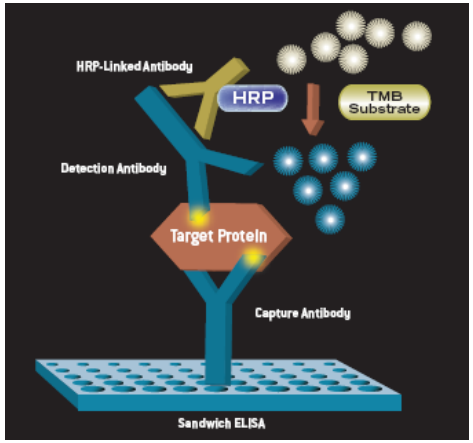

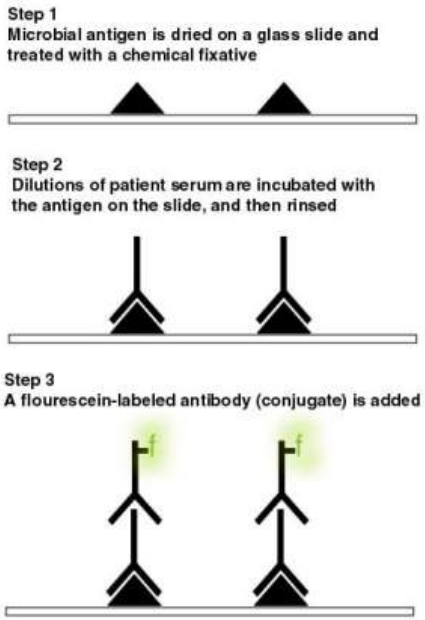

Androgen Resistance in Squirrel Monkeys (*Saimiri* spp.)

Katherine L Gross,[2‡] Jenne M Westberry,[1,2,‡] Tina R Hubler,[2] Patti W Sadosky,[2] Ravinder J Singh,[3] Robert L Taylor,[3] Jonathan G Scammell[1,2,*]

The goal of this study was to understand the basis for high androgen levels in squirrel monkeys (*Saimiri* spp.). Mass spectrometry was used to analyze serum testosterone, androstenedione, and dihydrotestosterone of male squirrel monkeys during the nonbreeding (n = 7) and breeding (n = 10) seasons. All hormone levels were elevated compared with those of humans, even during the nonbreeding season; the highest levels occurred during the breeding season. The ratio of testosterone to dihydrotestosterone in squirrel monkeys is high during the breeding season compared to man. Squirrel monkeys may have high testosterone to compensate for inefficient metabolism to dihydrotestosterone. We also investigated whether squirrel monkeys have high androgens to compensate for low-activity androgen receptors (AR). The response to dihydrotestosterone in squirrel monkey cells transfected with AR and AR-responsive reporter plasmids was 4-fold, compared with 28-fold in human cells. This result was not due to overexpression of cellular FKBP51, which causes glucocorticoid and progestin resistance in squirrel monkeys, because overexpression of FKBP51 had no effect on dihydrotestosterone-stimulated reporter activity in a human fibroblast cell line. To test whether the inherently low levels of FKBP52 in squirrel monkeys contribute to androgen insensitivity, squirrel monkey cells were transfected with an AR expression plasmid, an AR-responsive reporter plasmid, and a plasmid expressing FKBP52. Expression of FKBP52 decreased the EC_{50} or increased the maximal response to dihydrotestosterone. Therefore, the high androgen levels in squirrel monkeys likely compensate for their relatively low 5α-reductase activity during the breeding season and AR insensitivity resulting from low cellular levels of FKBP52.

Abbreviations: AR, androgen receptor; GR, glucocorticoid receptor; LC-MS/MS, liquid chromatography–tandem mass spectrometry; MMTV, mouse mammary tumor virus; PR, progesterone receptor

Note related article on page180

Interstitial Myocardial Fibrosis in a Captive Chimpanzee (*Pan troglodytes*) Population

Michael L Lammey,[1,*] Gary B Baskin,[2] Andrew P Gigliotti,[3] D Rick Lee,[1] John J Ely,[1] and Meg M Sleeper[4]

The clinical and necropsy records of 36 (25 male and 11 female) chimpanzees age 10 to 40 y old that died over a 6-y period (2001 to 2006) were reviewed. All animals had annual physical exams that included electrocardiograms and serial blood pressures. Nine of the 36 animals had a complete cardiac evaluation by a board certified veterinary cardiologist, and 7 of the 36 animals (19%) were diagnosed with some form of cardiomyopathy. Systemic hypertension was noted in 3 cases. Cardiac arrhythmias (ventricular ectopy) were seen in 15 (12 male and 3 female) of the 36 animals (42%). Sudden cardiac death (SCD) occurred in 13 (11 male and 2 female) chimps (36%) and was the leading cause of death (n = 13), followed by renal failure (n = 9) and septicemia (n = 3). Histologic examination of the hearts revealed interstitial myocardial fibrosis (IMF) in 29 chimpanzees (81%), and all of the animals that died suddenly due to cardiac causes had IMF to varying degrees. More data will be needed to identify the possible causes of IMF in captive chimpanzees, and IMF may be associated with arrhythmias and SCD in these animals.

Abbreviations: APF, Alamogordo Primate Facility; ECG, electrocardiography; IMF, interstitial myocardial fibrosis; SCD, sudden cardiac death

- What is the most common clinical presentation of chimpanzees with interstitial myocardial fibrosis?
  1. Signs associated with renal failure
  2. Sudden death
  3. Signs associated with septicemia
  4. Signs associated with a cerebral infarct
  5. Signs associated with liver disease

- What is the most common clinical presentation of chimpanzees with interstitial myocardial fibrosis?
  1. Signs associated with renal failure
  2. **Sudden death (page 392)**
  3. Signs associated with septicemia
  4. Signs associated with a cerebral infarct
  5. Signs associated with liver disease

Lateral Femoral Hernias in a Line of FVB/NHsd Mice: A New Confounding Lesion Linked to Genetic Background?

Marilène Paquet,[1,*] Janice Penney,[2] and Derek Boerboom[3]

Several strains of transgenic mice derived from an inbred FVB/NHsd colony developed large masses on 1 or both flanks. Although originally suspected to be a phenotypic anomaly related to genetic modifications, nontransgenic littermates subsequently were affected with equal frequency, inculpating the FVB/NHsd founder colony. The masses were subcutaneous, soft, and exophytic and appeared over the course of a few weeks. Female mice were affected more frequently than males. Gross examination revealed the masses to consist of uni- or bilateral hernias of variable size, occasionally containing small or large intestine (or both), cecum, mesenteric adipose tissue, male reproductive organs, and ureters. All hernial sacs pouched through the femoral triangle laterally to the femoral vessels and therefore were classified as lateral femoral hernias. Lateral femoral hernias have not previously been described in the veterinary literature and have never been described as background lesions in a strain of mice. Our findings suggest likely genetic drift in this strain of FVB/NHsd mice, causing a background lesion that confounded phenotypic analyses of transgenic mice derived from this strain.

Note

- FVB/N mouse strain
- Incidence Female:Male = 7:1

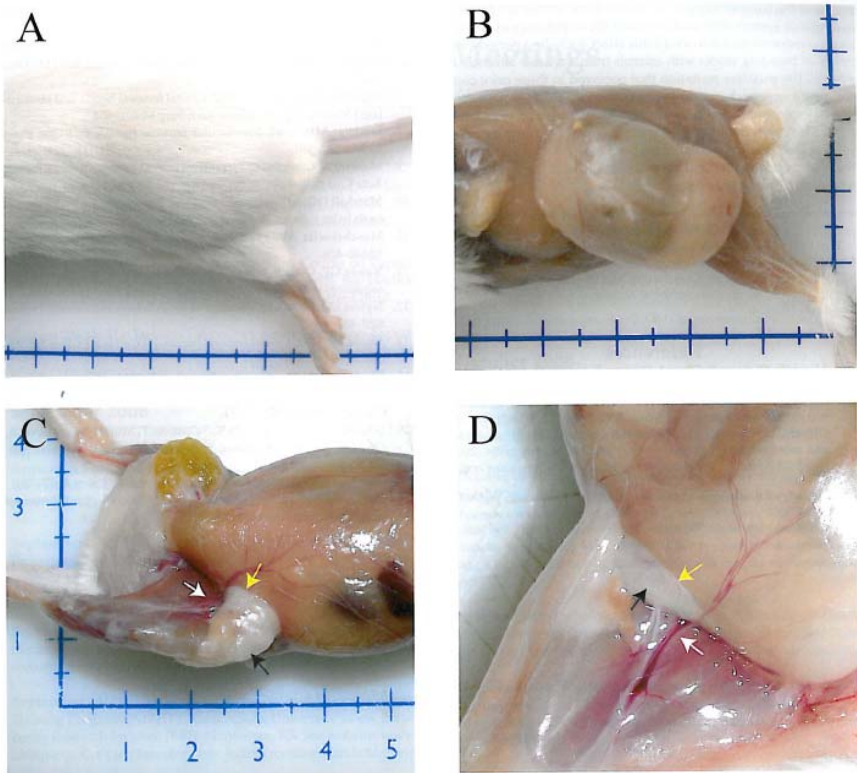

Volume 58(5)
October, 2008

The Laboratory Rat as an Animal Model for Osteoporosis Research

Pavlos P Lelovas,[1] Theodoros T Xanthos,[2] Sofia E Thoma,[1] George P Lyritis,[1] and Ismene A Dontas[1,2,*]

Osteoporosis is an important systemic disorder, affecting mainly Caucasian women, with a diverse and multifactorial etiology. A large variety of animal species, including rodents, rabbits, dogs, and primates, have been used as animal models in osteoporosis research. Among these, the laboratory rat is the preferred animal for most researchers. Its skeleton has been studied extensively, and although there are several limitations to its similarity to the human condition, these can be overcome through detailed knowledge of its specific traits or with certain techniques. The rat has been used in many experimental protocols leading to bone loss, including hormonal interventions (ovariectomy, orchidectomy, hypophysectomy, parathyroidectomy), immobilization, and dietary manipulations. The aim of the current review is not only to present the ovariectomized rat and its advantages as an appropriate model for the research of osteoporosis, but also to provide information about the most relevant age and bone site selection according to the goals of each experimental protocol. In addition, several methods of bone mass evaluation are assessed, such as biochemical markers, densitometry, histomorphometry, and bone mechanical testing, that are used for monitoring and evaluation of this animal model in preventive or therapeutic strategies for osteoporosis.

Abbreviations: BMD, bone mineral density; DEXA, dual-energy X-ray absorptiometry; μCT, microcomputerized tomography; pQCT, peripheral quantitative computerized tomography

- The rat skeletal system lacks which feature?
  1. A well-developed Haversian canal system
  2. A well-developed Volkmann’s canal system
  3. A well-developed endosteum
  4. A well-developed periosteum
  5. A well-developed cortex

- The rat skeletal system lacks which feature?
  1. **A well-developed Haversian canal system (page 425)**
  2. A well-developed Volkmann’s canal system
  3. A well-developed endosteum
  4. A well-develooped periosteum
  5. A well-developed cortex

Plasma Levels of Nitrite and Nitrate in Early and Recent Classes of Fish

Donna A Williams,[1,*] Mary H Flood,[1] Debra A Lewis,[2] Virginia M Miller,[3] and William J Krause[4]

The stable metabolite of nitric oxide in plasma is NO_x, the sum of nitrite plus nitrate. Measures of plasma NO_x may provide information about the nitric oxide tonus of the entire endothelium including capillary microvessels. Although data are available for mammalian species, plasma NO_x measurements in early vertebrate species are scarce. The purpose of this study was to test the hypothesis that plasma NO_x would be similar to the NO_x in the water environment for fish in early classes (Agnatha and Chondrichthye) and would exceed water NO_x levels in the known nitrite-sensitive fish (Osteichthye). Plasma samples were obtained from 18 species of adult fish (n = 167) and from their housing or natural water environment. NO_x was measured by using chemiluminescence. Plasma NO_x was detected in all species and ranged from 0.5 nmol/ml (skate) to 453.9 nmol/ml (shortnose gar). Average plasma NO_x was significantly higher in sea lamprey than in Atlantic hagfish whereas that of little skate was 3-fold lower than in spiny dogfish shark. Plasma NO_x differed significantly among early bony fish (paddlefish, pallid sturgeon, gar) yet was similar among modern bony fish, with the exception of rainbow trout. Plasma NO_x reflected water NO_x in only 2 species (hagfish and shark), and levels did not coincide with nitrite sensitivity. This study provides an expanded comparative view of plasma NO_x levels across 3 groups of early fish. The data obtained suggest a nitric oxide system in early and modern fish.

Abbreviation: NOS, nitric oxide synthase

Study of a *Bordetella hinzii* Isolate from a Laboratory Mouse

Nobuhito Hayashimoto,* Masahiko Yasuda, Kazuo Goto, Akira Takakura, and Toshio Itoh

Bordetella hinzii isolated from the trachea and lungs of a laboratory mouse with a respiratory infection was identified based on its phenotypic and genetic traits. The mouse showed sneezing with a chattering sound but without nasal discharge, and histopathologic examination revealed rhinitis, tracheitis, and bronchopneumonia. The isolate was a gram-negative, oxidase- and catalase-positive, short rod-shaped organism that produced alkali from malonate. The results of biochemical identification, an alkali production test from malonate, and partial sequence analysis of the 16S rRNA gene (1523 bp) were consistent with those reported previously for *B. hinzii*. The isolate induced sneezing in ICR mice and sneezing and slight to severe dyspnea in NOD-SCID mice after experimental infection. Histopathologic examination revealed catarrhal rhinitis and bronchopneumonia in both strains of mice and interstitial pneumonia in NOD-SCID mice. In light of these findings, *B. hinzii* was deemed to be a novel causative agent of respiratory disease in mice. This report describes the first isolation of *B. hinzii* from a mouse and confirms the organism's pathogenicity in mice.

Helicobacter Infection Decreases Reproductive Performance of IL10-deficient Mice

Julie M Sharp,[1] Deborah A Vanderford,[1] Maciej Chichlowski,[2] Matthew H Myles,[3] and Laura P Hale[2,*]

Infections with a variety of *Helicobacter* species have been documented in rodent research facilities, with variable effects on rodent health. *Helicobacter typhlonius* has been reported to cause enteric disease in immunodeficient and IL10$^{-/-}$ mice, whereas *H. rodentium* has only been reported to cause disease in immunodeficient mice coinfected with other *Helicobacter* species. The effect of *Helicobacter* infections on murine reproduction has not been well studied. The reproductive performance of C57BL/6 IL10$^{-/-}$ female mice intentionally infected with *H. typhlonius*, *H. rodentium*, or both was compared with that of age-matched uninfected controls or similarly infected mice that received antihelicobacter therapy. The presence of *Helicobacter* organisms in stool and relevant tissues was detected by PCR assays. *Helicobacter* infection of IL10$^{-/-}$ female mice markedly decreased pregnancy rates and pup survival. The number of pups surviving to weaning was greatest in noninfected mice and decreased for *H. rodentium* > *H. typhlonius* >> *H. rodentium* and *H. typhlonius* coinfected mice. *Helicobacter* organisms were detected by semiquantitative real-time PCR in the reproductive organs of a subset of infected mice. Treatment of infected mice with a 4-drug regimen consisting of amoxicillin, clarithromycin, metronidazole, and omeprazole increased pregnancy rates, and pup survival and dam fecundity improved. We conclude that infection with *H. typhlonius*, *H. rodentium*, or both decreased the reproductive performance of IL10$^{-/-}$ mice. In addition, antihelicobacter therapy improved fecundity and enhanced pup survival.

Abbreviation: qPCR, qualitative real-time PCR

- Mice of the B6.129P2-*Il10*^{tm1Cgn} genotype exhibit what inflammatory phenotype?
  1. Muted
  2. Exaggerated
  3. Absent
  4. Prolonged
  5. Shortened

- Mice of the B6.129P2-*Il10*^{tm1Cgn} genotype exhibit what inflammatory phenotype?
  1. Muted
  2. **Exaggerated (page 447)**
  3. Absent
  4. Prolonged
  5. Shortened

Lab codes:
http://dels.nas.edu/ilar_n/ilarhome/search_lc.php

Discrimination of Auditory Stimuli during Isoflurane Anesthesia

Manuel J Rojas,[1,†] Jinna A Navas,[1] Stephen A Greene,[2] and David M Rector[1,*]

Deep isoflurane anesthesia initiates a burst suppression pattern in which high-amplitude bursts are preceded by periods of nearly silent electroencephalogram. The burst suppression ratio (BSR) is the percentage of suppression (silent electroencephalogram) during the burst suppression pattern and is one parameter used to assess anesthesia depth. We investigated cortical burst activity in rats in response to different auditory stimuli presented during the burst suppression state. We noted a rapid appearance of bursts and a significant decrease in the BSR during stimulation. The BSR changes were distinctive for the different stimuli applied, and the BSR decreased significantly more when stimulated with a voice familiar to the rat as compared with an unfamiliar voice. These results show that the cortex can show differential sensory responses during deep isoflurane anesthesia.

Abbreviations: BSR, burst suppression ratio; EEG, electroencephalogram; GABA, γ-aminobutyric acid; MAC, minimum alveolar anesthetic concentration

Differential Susceptibility of SD and CD Rats to a Novel Rat Theilovirus

Michael T Drake,* Lela K Riley, and Robert S Livingston

Antibodies to rat theilovirus (RTV) have been detected in rats for many years because of their serologic crossreactivity with strains of Theiler murine encephalomyelitis virus (TMEV) of mice. Little information exists regarding this pathogen, yet it is among the most common viruses detected in serologic surveys of rats used in research. In the study reported here, a novel isolate of RTV, designated RTV1, was cultured from the feces of infected rats. The RTV1 genome contained 8094 nucleotides and had approximately 95% identity with another rat theilovirus, NSG910, and 73% identity with TMEV strains. In addition, the genome size of RTV1 was similar to those of TMEV strains but larger than that reported for NSG910. Oral inoculation of Sprague–Dawley (SD) and CD male rats (n = 10 each group) with RTV1 revealed that SD rats were more susceptible than CD rats to RTV1 infection. At 14 d postinoculation, 100% of SD rats shed virus in the feces, and 70% were positive for RTV serum antibodies. By 56 d postinoculation 30% of SD rats continued to have detectable virus in the feces, and 90% had seroconverted. In contrast, in inoculated CD rats RTV was detected only in the feces at 14 d postinoculation, at which time 40% of CD rats were fecal positive. By 56 d postinoculation only 20% of CD rats had detectable RTV serum antibodies. Our data provide additional sequence information regarding a rat-specific *Cardiovirus* and indicate that SD rats are more susceptible than CD rats to RTV1 infection.

Abbreviations: RACE, rapid amplification of cDNA ends; RTV, rat theilovirus; SD, Sprague Dawley; TMEV, Theiler murine encephalomyelitis virus

- To what family does rat theilovirus belong?
  1. Herpesviridae
  2. Picornaviridae
  3. Paramyxoviridae
  4. Parvoviridae
  5. Coronaviridae

- To what family does rat theilovirus belong?
  1. Herpesviridae
  2. **Picornaviridae (page 458)**
  3. Paramyxoviridae
  4. Parvoviridae
  5. Coronaviridae

Pathologic Findings in Rabbit Models of Hereditary Hypertriglyceridemia and Hereditary Postprandial Hypertriglyceridemia

Yoko Mitsuguchi,[1] Tsunekata Ito,[2] and Kazuo Ohwada[1,*]

In recent years, the association between hyperlipidemia and the development of arteriosclerosis has been addressed in several studies. Rabbit models of hypertriglyceridemia (TGH) and postprandial hypertriglyceridemia (PHT) have been developed at the authors' institute. TGH rabbits manifest pathology similar to that of humans with TGH, such as xanthoma, in addition to atherosclerosis of arterioles. Furthermore, PHT rabbits show visceral obesity, insulin resistance, and impaired glucose tolerance, with pathologic features similar to those of the metabolic syndrome assumed to be the cause of human ischemic heart disease. This study was designed to investigate the histopathologic features of TGH and PHT rabbits. TGH rabbits showed advanced aortic atherosclerosis, accompanied by intimal thickening of coronary and renal arteries, fatty liver changes, and xanthoma. PHT rabbits demonstrated aortic intimal thickening and hepatic fatty degeneration. The results of this study suggest that TGH and PHT rabbits are useful animal models for studying human hyperlipidemia and metabolic syndrome and the cardiovascular diseases that result from these conditions.

Abbreviations: LDL, low-density lipoprotein; PHT, postprandial hypertriglyceridemia; TGH, high triglyceride

Platelets from Diabetic Pigs Exhibit Hypersensitivity to Thrombin

Shivendra D Shukla,* Sanjay V Kansra,† MA Reddy, Sundeep M Shukla, David M Klachko, and Michael Sturek‡

Responses of platelets from diabetic and diabetic–hyperlipidemic pigs were studied. Pigs were made diabetic with single dose of alloxan, which acts by selectively destroying insulin-producing pancreatic β cells thus inducing type 1 diabetes. Pigs were kept for 1 or 12 wk, during which thrombin-induced aggregation was monitored in washed platelets. The platelets showed increased sensitivity to aggregation within 1 wk of induction of diabetes. Hyperlipidemia alone for 12 wk did not increase platelet hypersensitivity, but hyperlipidemia together with diabetes significantly increased thrombin-induced platelet aggregation. Because this hypersensitivity occurred in washed platelets, this characteristic appears to be independent of any contribution by plasma factors or other blood cells. The hypersensitivity of platelets from diabetic pigs correlated with decreased activity of mitogen-activated protein kinase. These studies offer the first evidence that platelet hyperactivity occurs during the early stages (within a week) of induction of diabetes in pigs and before manifestation of other cardiovascular problems.

Abbreviation: MAPK, mitogen-activated protein kinase

- Alloxan is used to induce what disease in pigs?
  1. Hyperthyroidism
  2. Hypothyroidism
  3. Hyperadrenocorticism
  4. Type I diabetes mellitus
  5. Type II diabetes mellitus

- Alloxan is used to induce what disease in pigs?
  1. Hyperthyroidism
  2. Hypothyroidism
  3. Hyperadrenocorticism
  4. **Type I diabetes mellitus (page 481)**
  5. Type II diabetes mellitus

Daily Rhythms of Serum Lipids in Dogs: Influences of Lighting and Fasting Cycles

Cristiano Bertolucci,[1] Francesco Fazio,[2] and Giuseppe Piccione[2,*]

Circadian clocks organize a wide array of metabolic functions in a coherent daily schedule and ensure synchrony of this schedule with environmental rhythms. Daily rhythmicity of lipid metabolism occurs in rodents and ruminants. We examined daily level variations of serum lipids (nonesterified fatty acids [NEFA], triglycerides, phospholipids, total cholesterol and total lipids) in healthy dogs, particularly focusing on their temporal relationship to lighting and fasting cycles. Whereas serum NEFA levels did not change across the day, levels of total lipids, total cholesterol, phospholipids, and triglycerides occurred in dogs maintained under 12:12-h light:dark cycles and fed a single meal daily. Only the rhythmic pattern of triglycerides responded to a 6 h delay in light onset, suggesting a cardinal role of a light-entrained circadian oscillator in its generation. To investigate whether temporal variations in serum lipids depend to physiological postprandial changes, we measured lipid levels in fasted dogs. Rhythms of total lipids, total cholesterol, phospholipids, and triglycerides vanished when dogs were food-deprived, indicating that these rhythms are driven by the digestive process. Levels of serum NEFA patterns were significantly higher during fasting than after food intake. The increase of NEFA concentrations during fasting may reflect the mobilization of adipose tissue NEFA mediated by the decrease in insulin with its lypolitic effects. Elucidating the daily rhythmicity of lipid levels is fundamental to understanding the metabolism of the dog, an animal model frequently used for research in metabolic pathophysiology.

Abbreviation: NEFA, nonesterified fatty acids

A Canine Model of Sustained Atrial Fibrillation Induced by Rapid Atrial Pacing and Phenylephrine

Anusak Kijtawornrat,[1,2] Brian M Roche,[1] and Robert L Hamlin[1,2,*]

Atrial fibrillation is a common arrhythmia with considerable morbidity and mortality. Limitations in studying both the mechanisms and therapy of atrial fibrillation arise due to the paucity of models that yield sufficiently high-quality data, are not costly, and in which atrial fibrillation is sustained long enough to make the necessary observations. The canine model we present is based on the hypothesis that atrial fibrillation requires heterogeneity of repolarization, that distribution of vagal fibers is heterogeneous in the atria, and that atrial fibrillation will persist after reflex stimulation of vagal efferents by increased systemic arterial pressure. Dogs were anesthetized with morphine–chloralose because this combination maintains nearly intact autonomic control. Systemic arterial pressure was elevated approximately 75 mm Hg during infusion of phenylephrine (2 $\mu g/kg \cdot min^{-1}$). The right atrium was paced for 20 min at 40 Hz. Atrial fibrillation was sustained after cessation of atrial pacing in dogs receiving phenylephrine, but terminated within seconds in normotensive animals. In conclusion, atrial fibrillation can be maintained for at least 40 min after cessation of rapid atrial pacing in dogs with phenylephrine-induced hypertension.

Volume 58 (6)

December 2008

Murine Norovirus: An Intercurrent Variable in a Mouse Model of Bacteria-Induced Inflammatory Bowel Disease

Karen Chase Lencioni,[1,*] Audrey Seamons,[2] Piper M Treuting,[2] Lillian Maggio-Price,[2] and Thea Brabb[2]

Murine norovirus (MNV) has recently been recognized as a widely prevalent viral pathogen in mouse colonies and causes disease and mortality in mice with impaired innate immunity. We tested the hypothesis that MNV infection would alter disease course and immune responses in mice with inflammatory bowel disease (IBD). FVB.129P2-*Abcb1a*^{tm1Bor} N7 (*Mdr1a*−/−) mice develop spontaneous IBD that is accelerated by infection with *Helicobacter bilis*. As compared with controls, *Mdr1a*−/− mice coinfected with MNV4 and *H. bilis* showed greater weight loss and IBD scores indicative of severe colitis, demonstrating that MNV4 can modulate the progression of IBD. Compared with controls, mice inoculated with MNV4 alone had altered levels of serum biomarkers, and flow cytometric analysis of immune cells from MNV4-infected mice showed changes in both dendritic cell (CD11c$^+$) and other nonT cell (CD4$^-$ CD8$^-$) populations. Dendritic cells isolated from MNV4-infected mice induced higher IFNγ production by polyclonal T cells in vitro at 2 d after infection but not at later time points, indicating that MNV4 infection enhances antigen presentation by dendritic cells early after acute infection. These findings indicate that acute infection with MNV4 is immunomodulatory and alters disease progression in a mouse model of IBD.

Abbreviations: DC, dendritic cell; IBD, inflammatory bowel disease; IP, IFNγ-inducible protein; MCP, macrophage chemotactic protein; MLN, mesenteric lymph node; MNV, murine norovirus; TNF, tumor necrosis factor

Note

- Norovirus in family Caliciviridae
  - ssRNA
- RAG -/- mice
  - Lack what cells?
- *Helicobacter bilis*
  - IBD in SCID mice
- IcrTac:ICR mice
  - Colon indicates what?

Helicobacter typhlonius and *Helicobacter rodentium* Differentially Affect the Severity of Colon Inflammation and Inflammation-Associated Neoplasia in IL10-Deficient Mice

Maciej Chichlowski,[1] Julie M Sharp,[2] Deborah A Vanderford,[2] Matthew H Myles,[3] and Laura P Hale[1,*]

Infection with *Helicobacter* species is endemic in many animal facilities and may alter the penetrance of inflammatory bowel disease (IBD) phenotypes. However, little is known about the relative pathogenicity of *H. typhlonius*, *H. rodentium*, and combined infection in IBD models. We infected adult and neonatal IL10$^{-/-}$ mice with *H. typhlonius*, *H. rodentium*, or both bacteria. The severity of IBD and incidence of inflammation-associated colonic neoplasia were assessed in the presence and absence of anti*Helicobacter* therapy. Infected IL10$^{-/-}$ mice developed IBD with severity of noninfected (minimal to no inflammation) < *H. rodentium* < *H. typhlonius* < mixed *H. rodentium* + *H. typhlonius* (severe inflammation). Inflammation-associated colonic neoplasia was common in infected mice and its incidence correlated with IBD severity. Combined treatment with amoxicillin, clarithromycin, metronidazole, and omeprazole eradicated *Helicobacter* in infected mice and ameliorated established IBD in both infected and noninfected mice. Infection of IL10$^{-/-}$ mice with *H. rodentium*, *H. typhlonius*, or both organisms can trigger development of severe IBD that eventually leads to colonic neoplasia. The high incidence and multiplicity of neoplastic lesions in infected mice make this model well-suited for future research related to the development and chemoprevention of inflammation-associated colon cancer. The similar antiinflammatory effect of antibiotic therapy in *Helicobacter*-infected and -noninfected IL10$^{-/-}$ mice with colitis indicates that unidentified microbiota in addition to *Helicobacter* drive the inflammatory process in this model. This finding suggests a complex role for both *Helicobacter* and other intestinal microbiota in the onset and perpetuation of IBD in these susceptible hosts.

Abbreviation: IBD, inflammatory bowel disease.

Quantitative Tomography of Early-Onset Spontaneous AA Amyloidosis in Interleukin 6 Transgenic Mice

Jonathan S Wall,[1,*] Tina Richey,[1] Amy Allen, Robert Donnell,[2] Steve J Kennel,[1] and Alan Solomon[1]

Mice that constitutively express the human interleukin 6 (huIL6) protein from a heritable transgene (*H2-L^d-IL-6*) express high levels of the acute-phase reactant, serum amyloid protein A, a liver-derived apoprotein of high-density lipoprotein that is the precursor of AA amyloid. Typically at approximately 5 mo of age B6(C)- *Tg(H2-L^d-IL-6)Kish* (H2/huIL-6) animals begin to develop splenic deposits of AA amyloid, which progress to involve the liver, kidney, and vasculature, ultimately resulting in death due to severe systemic AA amyloidosis at 8 to 9 mo of age. These mice provide a robust model in which to study novel therapeutic and diagnostic imaging agents for AA amyloidosis. We recently have noted a change in onset of spontaneous disease, as evidenced by 2 female transgenic mice that were found moribund at only 5 mo of age. Extensive hepatosplenic amyloid deposits in both mice were identified and quantified by single-photon emission computed tomography, which further revealed heterogeneous distribution of radiotracer in the spleen indicating a distinction between amyloid-laden red pulp and the disease-free lymphoid follicles. The AA nature of the deposits was evidenced immunohistochemically and by mass spectrometric analyses of extracted amyloid fibrils. Our studies have documented the manifestation of early-onset, severe, spontaneous AA amyloidosis in 2- to 5-mo-old H2/huIL-6 mice; we hypothesize that this disease is due to genetic rather than environmental factors.

Abbreviations: au, arbitrary units; CT, computed tomography; huIL6, human interleukin 6; SAP, serum amyloid P; SPECT, single photon emission computed tomography; sAA, serum amyloid A.

- The tissue shown exhibits positive congo red staining. What material or tissue is indicated by this staining pattern?
  1. Collagen
  2. Skeletal muscle
  3. Bone
  4. Amyloid
  5. Mineralization

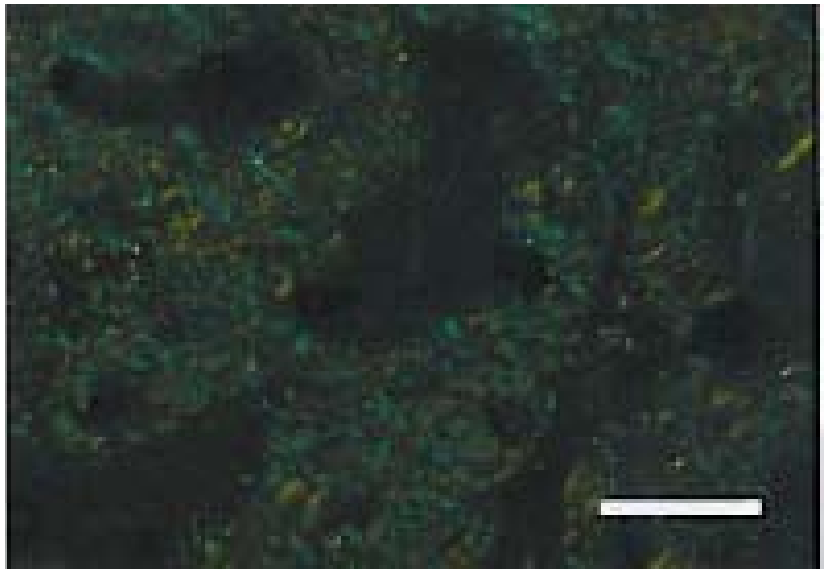

- The tissue shown exhibits positive congo red staining. What material or tissue is indicated by this staining pattern?
  1. Collagen
  2. Skeletal muscle
  3. Bone
  4. **Amyloid (page 543/544)**
  5. Mineralization

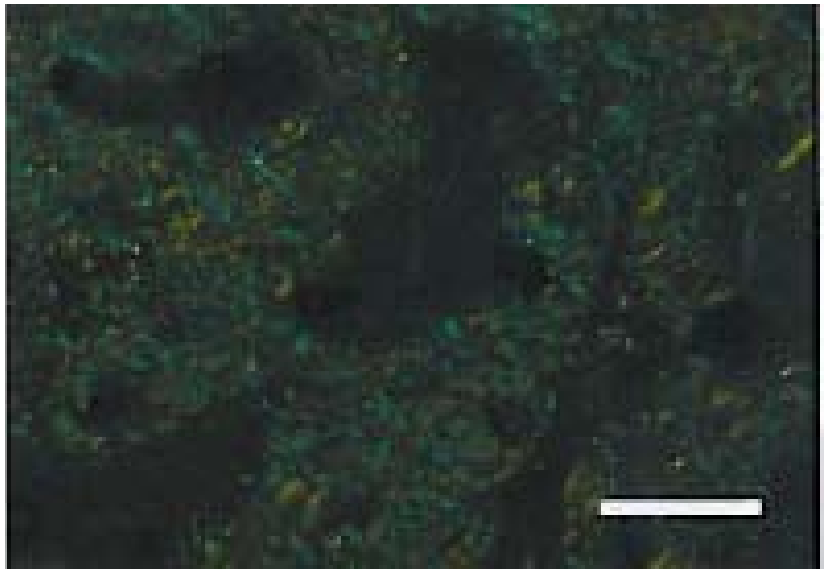

Note Also

- Transgenic denotation/nomenclature
- IL6 as pro-inflammatory cytokine
- SPECT and CT images:

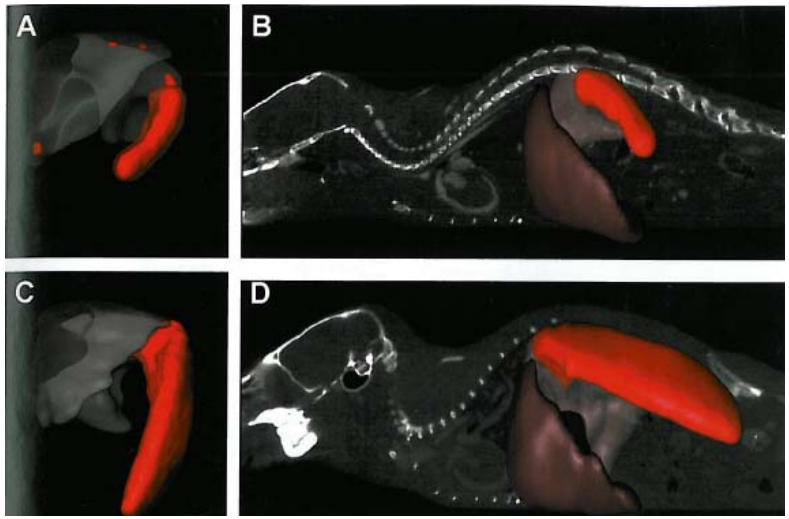

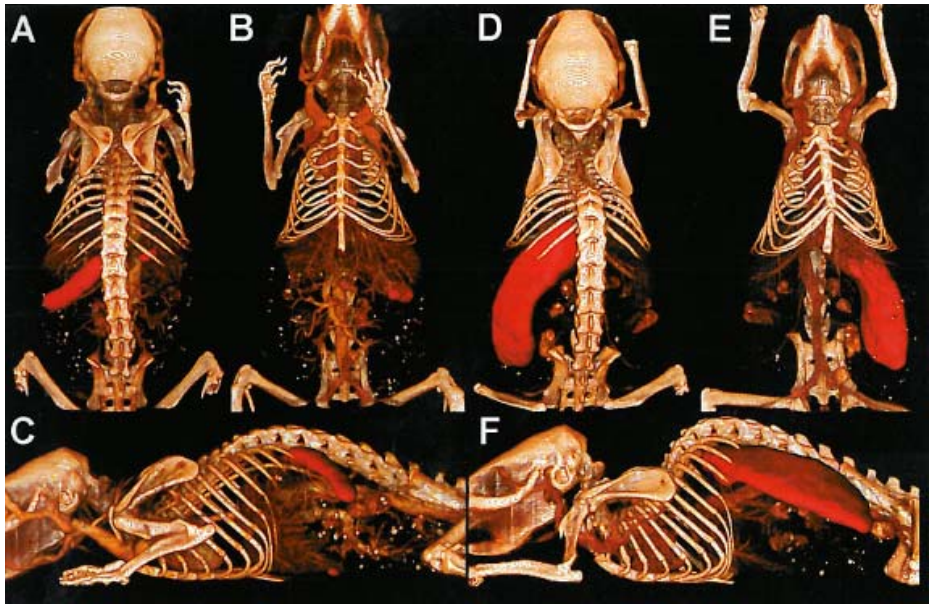

The Petit Rat (*pet/pet*), a New Semilethal Mutant Dwarf Rat with Thymic and Testicular Anomalies

Junko Chiba, Katsushi Suzuki, and Hiroetsu Suzuki*

The petit rat (*pet/pet*) is a recently discovered semilethal mutant dwarf. The neonatal *pet/pet* rats had a low body weight and small thymus and testis. During the first 3 d after birth, 50% of the male and 80% of the female *pet/pet* pups were lost or found dead. Surviving *pet/pet* rats showed marked retardation of postnatal growth, and their body weights were 41% (female rats) and 32% (male rats) of those of normal rats at the adult stage. The *pet/pet* rats exhibited proportional dwarfism, and their longitudinal bones were shorter than those of controls without skeletal malformations. Most organs of male *pet/pet* rats, especially the thymus, testis, adipose tissue surrounding the kidney, and accessory sex organs, weighed markedly less at 140 d of age than did those of their normal counterparts. The thymus of *pet/pet* rats was small with abnormal thymic follicles. Testes from *pet/pet* rats exhibited 2 patterns of abnormal histology. Spermatogenesis was present in testes that were only slightly anomalous, but the seminiferous tubules were reduced in diameter. In severely affected testes, most of the seminiferous tubules showed degeneration, and interstitial tissue was increased. Plasma growth hormone concentrations did not differ between *pet/pet* and normal male rats. The dwarf phenotype of *pet/pet* rats was inherited as an autosomal recessive trait. These results indicate that the *pet/pet* rat has a semilethal growth-hormone-independent dwarf phenotype that is accompanied by thymic and testicular anomalies and low birth weight.

Abbreviations: GH, growth hormone; PET, petit; TBS, Tris-HCl buffered saline.

Note

- Wistar-Imamichi rats
- Coisogenic
- Phenotype
  - Dwarfism, thymic atrophy, testicular anomalies, diminished growth hormone

Phenotypic Characterization of the Komeda Miniature Rat Ishikawa, an Animal Model of Dwarfism Caused by a Mutation in *Prkg2*

Atsuko Tsuchida,[1,*] Norihide Yokoi,[2,3] Misako Namae,[4] Masanori Fuse,[2] Taku Masuyama,[6] Masashi Sasaki,[7] Shoji Kawazu,[1] and Kajuro Komeda[5,+]

The Komeda miniature rat Ishikawa (KMI) is a spontaneous animal model of dwarfism caused by a mutation in *Prkg2*, which encodes cGMP-dependent protein kinase type II (cGKII). This strain has been maintained as a segregating inbred strain for the mutated allele *mri*. In this study, we characterized the phenotype of the KMI strain, particularly growth traits, craniofacial measurements, and organ weights. The homozygous mutant (*mri*/*mri*) animals were approximately 70% to 80% of the size of normal, heterozygous (*mri*/+) animals in regard to body length, weight, and naso-occipital length of the calvarium, and the retroperitoneal fat of *mri*/*mri* rats was reduced greatly. In addition, among progeny of the (BN×KMI-*mri*/*mri*)F1×KMI-*mri*/*mri* backcross, animals with the KMI phenotype (*mri*/*mri*) were easily distinguished from those showing the wild-type phenotype (*mri*/+) by using growth traits such as body length and weight. Genetic analysis revealed that all of the backcrossed progeny exhibiting the KMI phenotype were homozygous for the KMI allele in the 1.2-cM region between *D14Rat5* and *D14Rat80* on chromosome 14, suggesting strongly that *mri* acts in a completely recessive manner. The KMI strain is the first and only rat model with a confirmed mutation in *Prkg2* and is a valuable model for studying dwarfism and longitudinal growth traits in humans and for functional studies of cGKII.

Abbreviations: cGKII, cGMP-dependent protein kinase type II; CNP, C-type natriuretic peptide; KMI, Komeda miniature rat Ishikawa.

The Adult Göttingen Minipig as a Model for Chronic Heart Failure After Myocardial Infarction: Focus on Cardiovascular Imaging and Regenerative Therapies

Karl H Schuleri,[1,2,*] Andrew J Boyle,[3] Marco Centola,[1,2] Luciano C Amado,[1] Robert Evers,[1] Jeffrey M Zimmet,[1] Kristine S Evers,[1] Katherine M Ostbye,[1] Diana G Scorpio,[4] Joshua M Hare,[5] and Albert C Lardo[1,2]

Porcine models have become increasingly popular in cardiovascular research. The standard farm pig rapidly increases in body weight and size, potentially confounding serial measurements of cardiac function and morphology. We developed an adult porcine model that does not show physiologic increases in heart mass during the study period and is suitable for long-term study. We compared adult minipigs with the commonly used adolescent Yorkshire swine. Myocardial infarction was induced in adult Göttingen minipigs and adolescent Yorkshire swine by occlusion of the left anterior descending coronary artery followed by reperfusion. At 8 wk after infarction, the left ventricular ejection fraction was 34.1 ± 2.3% in minipigs and 30.7 ± 2.0% in Yorkshire swine. The left ventricular end-diastolic mass in Yorkshire pigs assessed by magnetic resonance imaging increased 17 ± 5 g, from 42.6 ± 4.3 g at week 1 after infarction to 52.8 ± 6.6 g at week 8, whereas it remained unchanged in minipigs. Cardiac anatomy and physiology in adult minipigs were evaluated invasively by angiography and noninvasively by Multidetector Computed Tomography and by Magnetic Resonance Imaging at 1.5 T and 3 T prior to myocardial infarction and during folow-up. This porcine heart failure model is reproducible, mimics the pathophysiology in patients who have experienced myocardial infarction, and is suitable for imaging studies. New heart failure therapies and devices can be tested preclinically in this adult animal model of chronic heart failure.

Abbreviations: CEMRA, contrast-enhanced magnetic resonance angiography; CI, confidence interval; ECG, electrocardiogram; LAD, left anterior descending artery; LV, left ventricle; LVEF, left ventricular ejection fraction; MDCT, multidetector computed tomography; MI, myocardial infarction; MRI, magnetic resonance imaging

- The coronary vasculature is similar in structure to 90% of the human population in what respect?
  1. The right coronary artery is dominant
  2. The left coronary artery is dominant
  3. The left circumflex artery is absent
  4. The right coronary artery supplies the left distal circumflex artery
  5. The left coronary artery supplies the right distal circumflex

- The coronary vasculature is similar in structure to 90% of the human population in what respect?
  1. **The right coronary artery is dominant (page 573)**
  2. The left coronary artery is dominant
  3. The left circumflex artery is absent
  4. The right coronary artery supplies the left distal circumflex artery
  5. The left coronary artery supplies the right distal circumflex

Bama Miniature Pigs (*Sus scrofa domestica*) as a Model for Drug Evaluation for Humans: Comparison of In Vitro Metabolism and In Vivo Pharmacokinetics of Lovastatin

Yu Liu, Ben-hua Zeng, Hai-tao Shang, Yan-yan Cen, and Hong Wei*

The objective of this study was to demonstrate that Bama miniature pigs are a suitable experimental animal model for the evaluation of drugs for man. To this end, in vitro lovastatin metabolism at the minipig liver microsomal level and in vivo pharmacokinetics were studied. Results were compared with those obtained from humans. Our data indicate that the main metabolites and enzyme kinetic parameters of lovastatin metabolism are similar in pigs and humans. Triacetyloleandomycin, a specific inhibitor of human CYP3A4, inhibited the metabolism of lovastatin in pig and human liver microsomes. In addition, the pharmacokinetic parameters and absolute bioavailability suggested that the absorption and elimination of lovastatin in Bama miniature pigs were similar to those in humans. Lovastatin was distributed across many organs in pigs, but the highest levels were found in the stomach, intestines, and liver. Within 96 h, 7% and 82% of the given dose was excreted in the urine and feces, respectively. In addition, no significant species differences in the plasma protein binding ratio of lovastatin and the rates of lovastatin hydrolysis to β-hydroxyacid lovastatin were apparent. From these results, we conclude that Bama miniature pigs are suitable for use in drug evaluation studies.

Abbreviations: CL_{int},intrinsic clearance; CYP, cytochrome P450; HA, β-hydroxyacid lovastatin; TAO, triacetyloleandomycin.

Can Gender Differences Be Evaluated in a Rhesus Macaque (*Macaca mulatta*) Model of Focal Cerebral Ischemia?

Stephanie J Murphy,[1,*] Jeffrey R Kirsch,[1] Wenri Zhang,[1] Marjorie R Grafe,[1,2] G Alex West,[3] Gregory J del Zoppo,[5] Richard J Traystman,[4] and Patricia D Hurn[1]

Gender differences, sex steroid effects, and sex-specific candidate therapeutics in ischemic stroke have been studied in rodents but not in nonhuman primates. In this feasibility study (n = 3 per group), we developed a model of transient focal cerebral ischemia in adult male and female rhesus macaques that consistently includes white matter injury. The animals also were used to determine whether gender-linked differences in histopathologic outcomes could be evaluated in this model in future, larger preclinical trials. Histologic brain pathology was evaluated at 4 d after 90 min of reversible occlusion of the middle cerebral artery (MCA). MCA occlusion was accomplished by using a transorbital approach and temporary placement of an aneurysm clip. Male and female rhesus macaques 7 to 11 y of age were studied. Baseline and intraischemic blood glucose, systolic blood pressure, heart rate, oxygen saturation, end-tidal CO_2, and rectal temperatures were not different among groups. The variability in injury volume was comparable to that observed in human focal cerebrovascular ischemia and in other nonhuman primate models using proximal MCA occlusion. In this small sample, the volume of injury was not different between male and female subjects, but observed variability was higher in female caudate nucleus, putamen, and hemisphere. This report is the first to compare cerebral ischemic outcomes in female and male rhesus macaques. The female rhesus macaque ischemic stroke model could be used after rodent studies to provide preclinical data for clinical trials in women.

Abbreviations: BP, blood pressure; $EtCO_2$, end-tidal CO_2, MCA, middle cerebral artery; SpO_2, oxygen saturation of peripheral blood.

Note

- Fluoro-Jade B
  - Fluoroscein derivative used to identify degenerative neurons

Effects of Maternal and Infant Characteristics on Birth Weight and Gestation Length in a Colony of Rhesus Macaques (*Macaca mulatta*)

Kelly J Hopper,[1,*] Denise K Capozzi,[2] and Joseph T Newsome[2]

A retrospective study using maternal and birth statistics from an open, captive rhesus macaque colony was done to determine the effects of parity, exposure to simian retrovirus (SRV), housing, maternal parity, and maternal birth weight on infant birth weight, viability and gestation length. Retrospective colony statistics for a 23-y period indicated that birth weight, but not gestation length, differed between genders. Adjusted mean birth weights were higher in nonviable infants. Mothers positive for SRV had shorter gestations, but SRV exposure did not affect neonatal birth weights or viability. Infants born in cages had longer gestations than did those born in pens, but neither birth weight nor viability differed between these groups. Maternal birth weight did not correlate with infant birth weight but positively correlated with gestation length. Parity was correlated with birth weight and decreased viability. Increased parity of the mother was associated with higher birth weight of the infant. A transgenerational trend toward increasing birth weight was noted. The birth statistics of this colony were consistent with those of other macaque colonies. Unlike findings for humans, maternal birth weight had little predictive value for infant outcomes in rhesus macaques. Nonviable rhesus infants had higher birth weights, unlike their human counterparts, perhaps due to gestational diabetes occurring in a sedentary caged population. Similar to the situation for humans, multiparity had a protective effect on infant viability in rhesus macaques.

Abbreviations: ANCOVA, analysis of covariance; PRL, Primate Research Laboratory; SRV, simian retrovirus.

Note

- Rhesus macaque reproductive physiology
  - Gestation length: 146 days
  - Menstrual cycle: 28 days

Dietary Supplementation with S-Adenosyl Methionine was Associated with Protracted Reduction of Seizures in a Line of Transgenic Mice

Sheryl Perry, James Levasseur, Amy Chan, and Thomas B Shea*

Transgenic mice, although useful for analyses of gene function, can present unanticipated phenotypic manifestations, including behavioral problems, that may not be directly associated with the gene of interest but rather due to the complex interplay inherent in genomes. These unexpected events can present unique insight into gene function, leading to an advantage in some situations, yet in others can confound interpretation and compromise usefulness of the transgenic line. Here we document that short-term supplementation with S-adenosyl methionine (SAM)—a nutriceutical known to regulate neurotransmitter levels, improve working memory, and reduce aggression—reduced handling- and startling-induced seizures that otherwise precluded behavioral analyses in a transgenic line. This effect lasted for at least 1 mo after withdrawal of SAM and allowed mice to be used in standard maze analyses. These findings suggest that short-term administration of a neurotropic nutriceutical may provide a functional rescue for behavioral studies in an otherwise intractable transgenic mouse line as well as improve the welfare of similar lines.

Abbreviations: SAH, S-adenosyl homocysteine; SAM, S-adenosyl methionine.

Note

- ApoE KO mouse nomenclature
- AIN-76 diet
  - What type of diet is this?
- Mazes
  - Y and 3 arm maze

Now…..

RELAX AND GO PASS THIS THING!!